THE COLLEGE OF AERONAUTICS

CRANFIELD

A PRELIMINARY REPORT ON THE DESIGN AND PERFORMANCE OF DUCTED WINDMILLS

by

G.M. LILLEY and W.J. RAINBIRD

THE COLLEGE OF AERONAUTICS

CRANFIELD

A preliminary report on the design and performance of
ducted windmills *

—by—

G.M. Lilley, M.Sc, D.I.C.

and

W.J. Rainbird, B.E., D.C.Ae.

of the Department of Aerodynamics

SUMMARY

A preliminary study is made of the theoretical gain
in power output obtained with a fully ducted land-type windmill
as compared with the standard unshrouded type windmill. The
design of the internal and external ducting is discussed
together with its effects on the overall performance of the
windmill. The differences in the aerodynamic design of the
blades for the ducted and unshrouded windmills are considered
and attention is drawn to the importance of the use of the
correct induced (or interference) velocities. A brief review
is included of recent Japanese theoretical and experimental
studies on ducted windmills.

The gain in performance is shown to be due to (a) a
reduction in the tip loss and (b) the effect of the increased
axial velocity through the windmill by controlled diffusion
of the slipstream. The gain is shown to depend critically
on the internal frictional losses, the diffuser expansion ratio
downstream of the windmill and the external shape of the duct
at exit and less on the inlet contraction ratio. It is found
that with suitable design of ducting the gain in power output
should be at least 65 per cent, as compared with the ideal
power output of an unshrouded windmill, if both the ducted
and unshrouded windmills are of the same diameter. Since the
disc loadings of the ducted windmill are very much lower than

those of the unshrouded windmill, and the risk of high gust loading will be less, it is suggested that the simplification in the design of the windmill will partly offset the increased cost due to the windmill ducting.

1. Index

Tables

2. Notation

a_o lift curve slope for blade

B number of blades

c chord

C_D drag coefficient

$C_E = \dfrac{E}{\frac{\rho}{2} V_o^3 \pi R_t^2}$ energy loss coefficient

$C_F = \dfrac{F}{\frac{\rho}{2} V_o^2 \pi R_t^2}$ axial force coefficient

C_L lift coefficient

$C_{p_4} = \dfrac{p_4 - p_o}{\frac{\rho}{2} V_o^2}$ pressure coefficient at duct outlet

$$C_P = \frac{P}{\frac{\rho}{2}V_o^3 \pi R_t^2} \quad \text{power coefficient}$$

C_P' maximum power coefficient of unshrouded windmill

$$C_x = \frac{C_L}{\sin \emptyset} + \frac{C_D}{\cos \emptyset}$$

$$C_y = \frac{C_L}{\cos \emptyset} - \frac{C_D}{\sin \emptyset}$$

D   drag

e   energy loss coefficient

E   energy loss in slipstream

E_D profile drag energy loss

f   disc loading of windmill

F   axial (drag) force on windmill

h_1, h_2 non-dimensional coefficients

H   total head, pitch of vortex sheets

$\triangle H$ loss of total head

I_o, I_1 Bessel functions ($I_o'(z) \equiv dI_o/dz$)

k   pressure drop coefficient, mass coefficient

K   rate of flow of kinetic energy, circulation function

K_o, K_1 Bessell functions

L   lift

m   integer, factor in drag integral

n   area ratio

p   pressure

$\triangle p$ mean pressure drop across windmill

P   power

q   resultant velocity

Q   torque

$r = \dfrac{C_P}{C_P^!}$ performance factor, $(r,\theta,z$ cylindrical coordinates)

R_i radius of windmill fairing

R_t outside radius of windmill blades

s element of length, non-dimensional parameter

S cross-sectional area

t time

u_r, u_θ, u_z velocity components

u axial component of velocity in slipstream or wake

v volume, velocity ratio

V axial component of velocity

V_o wind velocity

w_o velocity of rigid helicoidal vortex sheet

$\bar{w}_o = w_o / V_o$

W resultant velocity

x velocity ratio, radius ratio

X force

z velocity ratio, $(r,\theta,z$ cylindrical coordinates)

a blade incidence

a_o no lift angle

δ velocity increment ratio due to duct

η efficiency

θ blade angle, $(r,\theta,z$ cylindrical coordinates)

ϑ angle

$\mathcal{K}$ circulation function

μ reciprocal of diffuser expansion ratio, $\Omega\, r / V_o$

ρ density

σ solidity

$\emptyset$ velocity potential, relative flow angle

Γ circulation

$\triangle$ non-dimensional parameter

Ω angular velocity

Suffixes

1,2,3   denote sections of the duct

n,t   denote normal and tangential respectively

primes   denote conditions just downstream of the windmill

bar   denotes a ratio.

3. Introduction

This paper has been prepared at the suggestion of
Mr. Golding of the Electrical Research Association following
on some preliminary work done by one of the authors. It is
intended to be only a preliminary paper outlining the gains
in performance obtained with a ducted windmill over an un-
shrouded windmill, as well as the limits imposed on the
ducting and the design of the blades.

It is known, from the simple momentum theory of the
windmill, that for an unshrouded windmill the maximum power
output is only 59.3 per cent of the available kinetic energy
of the wind per unit time crossing an area equal to that
swept out by the blades. (In practice due to aerodynamic
losses this figure is reduced to about 40 per cent). Since
the action of the windmill in absorbing power from the wind
is to reduce the kinetic energy of the air passing through it,
it follows that only part of the available wind upstream of
the windmill actually flows through the windmill disc. This
energy, which is lost to the windmill, amounts to 40 per cent
of the available energy.

Various methods for increasing the power output from
windmills have been discussed by Betz[1]. These include the use
of multi-stage windmills and a combined propellor and windmill
in which the power to drive the propellor is provided by the
windmill. The propellor induces a higher axial velocity
through the windmill disc and thereby increases its power output.
Although the ducted, or axial flow, fan has been discussed by

many authors since 1920 the ducted windmill has received
little attention.   The first reference, known to the authors,
to the gain in power associated with the ducted over the
unshrouded windmill, is due to Vezzani[2].   A more complete
account of the performance of ducted windmills is due to
Sanuki[3] in which for the first time experimental results are
given.   Some further measurements are described by Iwasaki[4]
who also discusses the detailed aerodynamic design of
unshrouded and shrouded windmills.   Independently one of
the present authors[5] recently drew attention to the gain in
power output obtained with the fully ducted windmill.

        The ducted windmill, consisting of an entry cone, or
contraction, followed by a diffuser with the windmill operating
in the throat section, obtains its increased power output
from two independent effects.   These are (a) a reduction in
the tip loss and (b) a higher axial velocity through the wind-
mill disc   obtained by controlled diffusion of the slipstream.
The gain in performance due to (a) can only be found from a
complete analysis of the aerodynamic design of the windmill.
The experimental and theoretical work of Iwasaki[4] show however
that this gain in power output can amount to as much as 30
per cent of the power of the unshrouded windmill.[x]   Sanuki's[3]
experiments on ducted windmills of 1,2,3,4 and 6 blades over
a range of blade settings were performed with a windmill
mounted between entry and exit cones having diameters 1.3 and
1.1 respectively greater than the windmill diameter.   The gain
in power output was greatest for a 2-blader and least for a
6-blader although in the former case the unshrouded power
output was so small that the blades were probably stalled.
The effect of (b) can, at least qualitatively, be found from
an application of one-dimensional flow theory when the internal
and external duct losses are included.   The gain in power
output with suitable duct design is found to be very much
larger than in the former case and can amount to as much as
90 per cent of the power of the unshrouded windmill.   (In
practical installations, however, it seems unlikely that
the total power output of a ducted windmill will exceed twice
that of an unshrouded windmill of the same diameter).   The
experiments of Sanuki[3] show that with relatively crude ducting
and no effective slipstream diffusion the increase in power
output is about 86 per cent for a two-blader windmill and
somewhat less for windmills having larger numbers of blades,
although for the two-blader most of the gain in power arose
from an unstalling of the blades.

---

x   The experiments, due to Iwasaki, were done with a shroud
ring of length equal to about one third of the windmill
diameter.   The tests were done at relatively large blade angles
and consequently the power outputs were well below the maximum.

The aerodynamic design of the blades of the fully ducted windmill is not as simple as in the case of either the unshrouded windmill or the axial flow fan. In the latter cases the disc loading and the power output can be calculated on the basis of lifting line theory, once the induced, or interference, velocities due to the vortex sheets in the slipstream, are known. These can be calculated from Goldstein's[6] theory and the work of Lock and Yeatman[7], Kramer[8], Kawada[9], Moriya[10], Theordorsen[11], Abe[12] and Takeyama[13]. In the case of the fully ducted windmill the induced velocities are a function of the ducting around the tips of the windmill blades, the diffuser and conditions in the slipstream far downstream of the windmill and its surrounding duct. A simple analysis easily demonstrates how important a correct evaluation of the induced velocities is in the aerodynamic design of a ducted windmill.

Part I of this paper deals with the performance of the ducted windmill and its comparison with that of the unshrouded windmill on the basis of simple one-dimensional theory. Part II, on the other hand, discusses the comparative performances of ducted and unshrouded windmills using the vortex theory of windmills.

PART I

One-dimensional flow theory

4. Analysis

In the simple aerodynamic theory of windmills, the windmill is assumed to have an infinite number of blades, so that it effectively becomes a circular actuator disc over which the axial force is uniformly distributed. The rotation of the slipstream is neglected and the axial component of the velocity must be the same on both sides of the disc in order to satisfy continuity of flow. There is, however, a discontinuity in the pressure as the air flows across the disc. It is assumed that the velocity across any plane perpendicular to the windmill axis is uniform and steady and the flow incompressible. We will first find the power output from an unshrouded windmill and then secondly compare its power output with that of a ducted windmill of the type shown in figure 1.

4a. The unshrouded windmill[14]

The axial force, power output and efficiency can be obtained from an application of Bernoulli's equation and the laws of conservation of mass and momentum to the control surface ABCDEF (see figure 2). Since the rates of mass flow

across sections '0', '2', '3' must be equal we have

$$V_o S_o = V_2 S_2 = V_3 S_3 \qquad \dots\dots\dots(1)$$

where V is the axial velocity and S is the cross-sectional area normal to the windmill axis. Since the flows upstream and downstream of the disc are irrotational we may separately apply Bernoulli's equation to the motion in these two regions. Therefore the total head, H, in these two regions is respectively,

$$H_o = p_o + \tfrac{1}{2}\rho V_o^2 = p_2 + \tfrac{1}{2}\rho V_2^2 \left.\right)$$

and

$$H_3 = p_2' + \tfrac{1}{2}\rho V_2^2 = p_3 + \tfrac{1}{2}\rho V_3^2 \left.\right) \qquad \dots\dots\dots(2)$$

Since the pressure p_3 far downstream must equal p_o, the pressure difference across the actuator disc is

$$p_2 - p_2' = \tfrac{1}{2}\rho \, (V_o^2 - V_3^2) \qquad \dots\dots\dots(3)$$

and the axial (drag) force F acting on the windmill disc, of area S_2, is

$$F = (p_2 - p_2')S_2 = \tfrac{1}{2}\rho S_2 V_o^2 \left(1 - \frac{V_3^2}{V_o^2}\right) \qquad \dots\dots\dots(4)$$

If we apply the momentum equation to the control surface ABCDEF it can be shown that

$$F = X + p_o \, (S_o - S_3) + \rho \, V_2 S_2 \, (V_o - V_3)$$

where X is the integral of the pressure forces acting on the curved boundaries ABC and DEF due to the fluid outside the slipstream. It can be shown that

$$X = - p_o \, (S_o - S_3) \qquad \dots\dots\dots(5)$$

and then

$$F = \rho V_2 S_2 \, (V_o - V_3) \qquad \dots\dots\dots(6)$$

It follows from equations (4) and (6) that

$$V_2 = \frac{V_o + V_3}{2} \qquad \dots\dots\dots(7)$$

or $\qquad F = \rho \left(\dfrac{V_o + V_3}{2} \right) S_2 (V_o - V_3)$ $\qquad$ ....(4a)

where $\rho \left(\dfrac{V_o + V_3}{2} \right) S_2$ is the rate of mass flow through the windmill disc and $(V_o - V_3)$ is the difference between the velocities of flow far upstream and far downstream.

The decrease of kinetic energy of the fluid in the slipstream per unit time is

$$K = \tfrac{1}{2}\rho \left(\dfrac{V_o + V_3}{2} \right) S_2 \ (V_o^2 - V_3^2)$$

$$= F \left(\dfrac{V_o + V_3}{2} \right) \qquad\qquad ....(8)$$

which equals the work done by the fluid on the windmill, P.

If we define the power coefficient, C_P, as the ratio of the work done by the fluid on the windmill, to the rate of flow of kinetic energy, far upstream of the windmill, through an area equal to that swept out by the blades, then

$$C_P = \dfrac{P}{\tfrac{1}{2}\pi R_t^2 \rho V_o^3} \qquad\qquad ....(9)$$

(This is the general expression for the windmill power coefficient and is independent of the number of blades and the size of windmill boss). If we assume that $S_2 = \pi R_t^2$ where R_t is the outside radius of the windmill then

$$C_P = \dfrac{P}{\tfrac{1}{2}\rho S_2 V_o^3} = \dfrac{K}{\tfrac{1}{2}\rho S_2 V_o^3} = \dfrac{(1 + V_3/V_o)}{2} \left(1 - \dfrac{V_3^2}{V_o^2} \right)$$

$$............(10)$$

The maximum power coefficient $C_P \ (V_3/V_o)$ is obtained when

$$V_3/V_o = \tfrac{1}{3}$$

$$\left. \right\} \qquad\qquad ....(11)$$

giving $\qquad C_{P_{max}} = \dfrac{16}{27} = 0.593$

The disc loading, $f = \dfrac{F}{\tfrac{1}{2}\rho S_2 V_2^2}$, corresponding to maximum

power is

$$f = \frac{4(1-V_3/V_o)}{(1+V_3/V_o)} = 2 \qquad \dots\dots\dots\dots(12)$$

although the disc loading itself is a maximum when $V_3/V_o = 0$ and $f = 4$.

It should be noted that the definition of disc loading f is different from that of the axial force (drag) coefficient $C_F = F/\frac{1}{2}\pi R_t^2 V_o^2$. Thus when $S_2 = \pi R_t^2$

$$C_F = \left(1 - V_3^2/V_o^2\right) \qquad \dots\dots\dots\dots(13)$$

and at maximum power

$$(C_F)_{C_{P_{max}}} = 8/9 \qquad \dots\dots\dots\dots(14)$$

4b. The ducted windmill

(i) Frictional losses neglected

Let us consider the performance of a windmill mounted in a duct having a cylindrical external profile (see figure 3). Since the flow is frictionless the only losses are those in the windmill slipstream.

As the air flows through the duct its pressure is decreased by $\triangle p$ across the windmill. The axial force, F, on the windmill is given by

$$F = S_2 \triangle p \qquad \dots\dots\dots\dots(1)$$

where S_2 is the windmill disc area.

If we apply the momentum theorem to the control surface ABCD we can show that

$$F = \rho S_2 V_2 (V_o - V_\infty) - D \qquad \dots\dots\dots\dots(2)$$

where D is the drag on the duct due to the internal and external flows.

If we next apply the momentum theorem to the flow inside the slipstream it can be shown that

$$F = \rho S_2 V_2 (V_o - V_\infty) - \triangle p (S_1 - S_2) \qquad \dots\dots\dots\dots(3)$$

Equations (1) and (3) together give

$$\Delta p \, S_1 = \rho S_2 V_2 \, (V_o - V_\infty) \qquad \cdots\cdots\cdots\cdots(4)$$

and equations (2) and (3) show that the duct drag

$$D = \Delta p \, (S_1 - S_2) \qquad \cdots\cdots\cdots\cdots(5)$$

This simple expression for the duct drag arises from the fact that its external profile is cylindrical. Equation (5) is not true for external profiles other than cylindrical and in any case it is only true for inviscid flow.

If we apply Bernoulli's equation to the flow upstream and downstream of the windmill we get

$$\left.\begin{aligned} H_o &= p_o + \tfrac{1}{2}\rho V_o^2 = p_2 + \tfrac{1}{2}\rho V_2^2 \\[2mm] H_1 &= p_2' + \tfrac{1}{2}\rho V_2^2 = p_o + \tfrac{1}{2}\rho V_\infty^2 \end{aligned}\right\} \qquad \cdots\cdots\cdots\cdots(6)$$

and

These equations show that

$$\Delta p = p_2 - p_2' = H_o - H_1 = \tfrac{1}{2}\rho(V_o^2 - V_\infty^2) \qquad \cdots\cdots\cdots(7)$$

which together with equation (4) leads to

$$V_2 = \frac{S_1}{S_2} \left(\frac{V_o + V_\infty}{2}\right) \qquad \cdots\cdots\cdots\cdots(8)$$

or alternatively

$$V_2 = \frac{V_o + V_\infty}{2} + \frac{S_1 - S_2}{S_2} \left(\frac{V_o + V_\infty}{2}\right) \qquad \cdots\cdots\cdots(8a)$$

The first term on the right hand side gives the contribution to V_2 due to the windmill slipstream and the second term is the contribution due to the duct.

The work done on the <u>ducted windmill</u> by the air is, using equation (8) for V_2,

$$P = F \, V_2 = \Delta p S_2 V_2 = \Delta p S_1 \left(\frac{V_o + V_\infty}{2}\right) \qquad \cdots\cdots\cdots(9)$$

or the power output for a given value of $\triangle p$ is proportional to the rate of volume flow through the windmill disc.

Now for an <u>unshrouded windmill</u> of disc area S the power output is

$$P = \triangle p \, S \left(\frac{V_o + V_\infty}{2} \right) \qquad \ldots\ldots\ldots\ldots(10)$$

<u>Hence the power output from a ducted windmill, where the external profile is cylindrical, is equivalent to that from an unshrouded windmill, having (a) a disc area equal to the duct inlet (exit) area, and (b) the same pressure drop as the ducted windmill.</u>

When the external profile of the windmill duct is not cylindrical (figure 4) equations (1) and (2) still hold, but the duct drag, D, is given by

$$D = \int_E p \, dS - \int_I p \, dS \qquad \ldots\ldots\ldots\ldots(11)$$

where 'E' and 'I' denote the external and internal surfaces of the duct respectively.   Since the flow is one dimensional the velocities inside the duct upstream of the windmill will be equal to those at the corresponding section downstream. Due to the pressure drop $\triangle p$ across the windmill, the contribution to the internal drag, between the inlet and the section downstream of the windmill having the same area as the inlet, is equal to $\triangle p(S_1 - S_2)$.   Between this section and the exit the external and internal pressure difference changes from $\triangle p$ at the area S_1 to zero at S_3.   Hence a mean value for this part of the drag contribution is

$\triangle p \, \dfrac{(mS_3 - S_1)}{2}$, where m is less than unity, and the

total drag becomes therefore,

$$D = \triangle p \, (S_1 - S_2) + \triangle p \, \frac{(mS_3 - S_1)}{2} \qquad \ldots\ldots\ldots\ldots(12)$$

Since $F = \triangle p \, S_2$ we have, after some rearrangement

$$1 + D/F = \frac{m + S_1/S_3}{2 \, S_2/S_3} \qquad \ldots\ldots\ldots\ldots(12a)$$

and D is only positive when $\dfrac{mS_3 + S_1}{S_2} > 2.$

From equation (2) with the value of D from (12) we find that

$$\rho S_2 V_2 \, (V_o - V_\infty) = \triangle p \left(\frac{m\,S_3 + S_1}{2} \right) \qquad \cdots\cdots\cdots(13)$$

But from equation (7)

$$\triangle p = \tfrac{1}{2}\rho \, (V_o - V_\infty)(V_o + V_\infty) \qquad \cdots\cdots\cdots(14)$$

and therefore

$$V_2 = \frac{(mS_3 + S_1)}{2\,S_2} \left(\frac{V_o + V_\infty}{2} \right) \qquad \cdots\cdots\cdots(15)$$

or alternatively

$$V_2 = \frac{V_o + V_\infty}{2} + \left(\frac{mS_3 + S_1 - 2S_2}{2S_2} \right) \left(\frac{V_o + V_\infty}{2} \right) \quad \cdots\cdots(15a)$$

Since the power output is still given by

$$P = F \, V_2$$

we find that when V_2 is substituted from equation (15)

$$P = \triangle p \, \frac{(mS_3 + S_1)}{2} \left(\frac{V_o + V_\infty}{2} \right) \qquad \cdots\cdots\cdots(16)$$

Thus the equivalent unshrouded windmill must have a disc area of $\frac{(mS_3 + S_1)}{2}$. It should be pointed out, however, that this result is only very approximate and depends on the expression obtained for the duct drag (equation (12). However, in practical applications the use of the factor m is simpler than say expressing the fairing drag in terms of the maximum velocity on the external profile.

From equations (16) and (14) the power output can also be written as

$$P = \frac{\rho (mS_3 + S_1)}{8} \, (V_o + V_\infty)(V_o^2 - V_\infty^2) \qquad \cdots\cdots\cdots(17)$$

and the power coefficient, C_P, in terms of the windmill swept area, πR_t^2, and the upstream velocity, V_o is

$$C_P = 4 \, v^2 \frac{S_2}{\left(\frac{mS_3 + S_1}{2}\right)} \left(1 - v \frac{S_2}{\left(\frac{mS_3 + S_1}{2}\right)}\right) \qquad \dots\dots\dots\dots(18)$$

where $\quad S_2 = \pi R_t^2 \quad$ and $\quad v = \frac{V_2}{V_o}$.

In the following section the importance of the expansion ratio, $1/\mu = S_3/S_2$, and the pressure coefficient at exit, $C_{p_4} = \frac{p_4 - p_o}{\frac{1}{2}\rho V_o^2}$, are demonstrated. The connection between these parameters and the terms used above will now be found.

Since the external and internal pressures at exit are equal it follows that

$$C_{p_4} = \frac{V_\infty^2}{V_o^2} - v^2 \mu^2 \qquad \dots\dots\dots\dots(19)$$

But from equation (14)

$$\frac{\Delta p}{\frac{1}{2}\rho V_2^2} = \left(1 - \frac{V_\infty^2}{V_o^2}\right) \frac{1}{v^2} = f \qquad \dots\dots\dots\dots(20)$$

and hence from equations (19) and (20)

$$v^2 f = 1 - (\mu^2 v^2 + C_{p_4}) \qquad \dots\dots\dots\dots(21)$$

From equation (2) the disc loading

$$f = \frac{F}{\frac{1}{2}\rho V_2^2 \, S_2} = \frac{2}{v}\left(1 - \frac{V_\infty}{V_o}\right) - \frac{C_D}{v^2} \qquad \dots\dots\dots\dots(22)$$

where $\quad C_D = \frac{D}{\frac{1}{2}\rho \, V_o^2 \, S_2}$

If we substitute for V_∞/V_o from equation (20) then

$$v^2 f + C_D = f v^2 \cdot \left(\frac{2V_2}{V_o + V_\infty}\right) \qquad \dots\dots\dots\dots(23)$$

where
$$\frac{2V_2}{V_o + V_\infty} = \frac{2v\left[1 - \sqrt{1 - v^2 f}\right]}{fv^2} \qquad \dots\dots\dots\dots(24)$$

$$= \frac{2v\left[1 - \sqrt{\mu^2 v^2 + C_{p4}}\right]}{1 - (\mu^2 v^2 + C_{p_4})} \qquad \dots\dots\dots\dots(24a)$$

In terms of the drag coefficients, C_D, equation (12) becomes

$$C_D + fv^2 = fv^2 \left(\frac{mS_3 + S_1}{2S_2}\right) \qquad \dots\dots\dots\dots(25)$$

and therefore on comparing equations (23) and (25) it follows that

$$\frac{mS_3 + S_1}{2S_2} = \frac{m + S_1/S_3}{2\mu} = \frac{2v\left[1 - \sqrt{\mu^2 v^2 + C_{p4}}\right]}{1 - (\mu^2 v^2 + C_{p_4})} \quad \dots(26)$$

which after some rearrangement leads to

$$m = \frac{4\mu v\left[1 - \sqrt{\mu^2 v^2 + C_{p4}}\right]}{1 - \mu^2 v^2 - C_{p_4}} - \frac{S_1}{S_3} \qquad \dots\dots\dots\dots(27)$$

A knowledge of the value of m enables the disc area of the equivalent windmill to be determined.

A very simple result arises when $S_1 = S_3$. In this case equations (5) and (12) show that $m = 1$, and solving equation (27) for v gives

$$v = \frac{2 \pm \sqrt{1 + 3C_{p4}}}{3\mu} \qquad \dots\dots\dots\dots(28)$$

Thus if C_{p_4} is negative it cannot be more negative than $-\frac{1}{3}$ and not greater than zero (see below). These conditions refer to maximum and zero power respectively. The fact that values of C_{p_4} more negative than $-1/3$ are not permissible is a rather surprising but nevertheless a very important deduction. Similar restrictions exist on the values of μ and v. From equations (20) and (8)

$$\frac{V_{ro}}{V_o} = \sqrt{1 - fv^2} = 2\mu v - 1 \qquad \ldots\ldots\ldots\ldots(29)$$

or

$$fv^2 = 4\mu v (1 - v\mu) \qquad \ldots\ldots\ldots\ldots(30)$$

and μ, and v must lie in the restricted range given by

$$\frac{1}{2\mu} < v < \frac{1}{\mu} \quad \text{for positive values of } f \text{ and } V_\infty .$$

When $m \neq 1$ the general formulae, replacing equation (30) and (28) are respectively

$$fv^2 = \frac{16 \mu^2 v^2}{(m + S_1/S_3)^2} \left[\frac{m + S_1/S_3}{2\mu v} - 1 \right] \qquad \ldots\ldots(31)$$

and

$$v = \frac{\frac{4}{m+S_1/S_3} - \sqrt{1 + C_{p_4}\left\{ \left(\frac{4}{m+S_1/S_3}\right)^2 - 1\right\}}}{\mu \left\{ \left(\frac{4}{m+S_1/S_3}\right)^2 - 1\right\}} \qquad \ldots(32)$$

Similarly the equation for the power coefficient found from equation (18) is

$$C_P = 8 \left(\frac{m+S_1/S_3}{\mu}\right) \left\{ \frac{16 - (m+S_1/S_3)^2}{4 - \sqrt{16+(1-C_{p_4})(m+S_1/S_3)^2}} - 2\right\}$$

$$x \left\{ \frac{4 - \sqrt{16+(1-C_{p4})(m+S_1/S_3)^2}}{16 - (m+S_1/S_3)^2}\right\} \qquad \ldots\ldots\ldots\ldots(33)$$

Thus for positive values of f and v

$$\frac{m + S_1/S_3}{4\mu} < v < \frac{m + S_1/S_3}{2\mu}$$

and

$$- C_{p_4} < \frac{1}{\left\{ \left(\frac{4}{m+S_1/S_3}\right)^2 - 1\right\}}$$

To these relations we must add the condition for
positive drag (equation 12a) viz. $\frac{m}{\mu} + S_1/S_2 > 2$, although this
will always be satisfied no matter what values are used for
μ and S_1/S_2.

Although all these relations are modified to some
extent when friction effects are included nevertheless they
represent useful limiting values in preliminary design studies.

The important results obtained from this section are
as follows.-

(1) The interdependence of the windmill power output and
the fairing drag.

(2) The power output is proportional to the rate of
volume flow through the windmill disc for a given
disc loading.

(3) The velocity through the windmill disc is equal to the
slipstream and the duct contributions.

4b. (continued). The ducted windmill

(ii) Flow with frictional losses included (see figure 4)

The flow far upstream, of velocity V_o, enters the
duct inlet, of area S_1, with the velocity V_1. The flow is
accelerated in the contraction and flows past the windmill of
disc area S_2 with the velocity V_2. The pressure discontinuity
across the windmill actuator disc is equal to $p_2 - p_2'$. The
velocity decreases along the diffuser and leaves the exit, of
area S_3, with the velocity V_3. The velocity further
decreases downstream of the exit since the pressure p_3 at
the duct exit is less than the uniform stream pressure p_o.
The velocity reaches a final value V far downstream of the
duct exit.

In the external flow around the duct it will be
assumed that outside the duct boundary layer the total head is
constant and equal to its value far upstream. It will be
assumed that at the duct exit the pressure p_4 is constant
across the boundary layer and equal to the value p_3 inside
the duct. In general p_4 will be less than p_o.

Inside the duct we will assume that the total head loss in the boundary layer arising from the friction force at the wall is distributed over the complete duct cross-section i.e. complete mixing at each section is assumed. If c_f is the local skin friction coefficient acting on the element of surface of the duct of length ds and perimeter πD then the total head loss, $\triangle H$, between two sections of the duct is given by

$$\triangle H = \rho \, \frac{\pi}{2} \int_{1}^{2} c_f \, V^2 \, \frac{D}{S} \, ds$$

where from continuity $V = \dfrac{V_1 S_1}{S}$. If C_F is the mean coefficient of skin friction in the duct between sections 1 and 2 then

$$\frac{\triangle H}{\frac{1}{2}\rho \, V_1^2} = 4 \, C_F \int_{1}^{2} \left(\frac{D_1}{D}\right)^5 \, d\left(\frac{s}{D_1}\right)$$

where V_1 and D_1 are the velocity and diameter respectively at the section 1.

The following losses will be included,

$\triangle H_1$ the mean total head loss at entry

$\triangle H_2$ the mean total head loss in the contraction section including the losses across guide vanes and fan fairings

$\triangle H_3$ the mean total head loss in the diffuser.

If we apply Bernoulli's equation to the flow inside the slipstream and the duct we obtain

$$\left. \begin{aligned} H_o = p_o + \tfrac{1}{2}\rho V_o^2 &= p_1 + \tfrac{1}{2}\rho V_1^2 + \triangle H_1 \\ p_1 + \tfrac{1}{2}\rho V_1^2 &= p_2 + \tfrac{1}{2}\rho V_2^2 + \triangle H_2 \\ p_2 + \tfrac{1}{2}\rho V_2^2 &= p_2' + \tfrac{1}{2}\rho V_2^2 + \triangle H_2' \\ p_2' + \tfrac{1}{2}\rho V_2^2 &= p_3 + \tfrac{1}{2}\rho V_3^2 + \triangle H_3 \end{aligned} \right\} \quad \dots\dots\dots\dots(1)$$

But the loss in total head across the windmill $\triangle H_2'$

is found from the axial (drag) force on the windmill

$$F = S_2 (p_2 - p_2') = S_2 \triangle H_2' \qquad \dots\dots\dots(2)$$

and

$$f = \frac{F}{\frac{1}{2}\rho S_2 V_2^2} = \frac{\triangle H_2'}{\frac{1}{2}\rho V_2^2} \qquad \dots\dots\dots(3)$$

From equation (1) it can be shown that

$$\tfrac{1}{2}\rho(V_o^2 - V_3^2) = p_3 - p_o + \sum_{i=1}^{3} \triangle H_i + \triangle H_2'$$

but since $p_3 = p_4$ and writing

$$C_{p_4} = \frac{p_4 - p_o}{\frac{1}{2}\rho V_o^2} \;\; ; \;\; \frac{V_3}{V_2} = \frac{S_2}{S_3} = \mu \;\; ; \;\; \frac{V_2}{V_o} = v$$

then

$$(f + \mu^2)v^2 = 1 - C_{p_4} - \frac{\sum \triangle H_i}{\frac{1}{2}\rho V_o^2} \qquad \dots\dots\dots(4)$$

If further we put

$$h_1 = 1 - C_{p_4} - \frac{\triangle H_1}{\frac{1}{2}\rho V_o^2}$$

and

$$h_2 = \mu^2 + \frac{\triangle H_2}{\frac{1}{2}\rho V_2^2} + \frac{\triangle H_3}{\frac{1}{2}\rho V_2^2}$$

then equation (4) becomes

$$(f + h_2) v^2 = h_1 \qquad \dots\dots\dots(5)$$

and

$$v = \sqrt{\frac{h_1}{f + h_2}} \qquad \dots\dots\dots(6)$$

The power output [x] from the windmill is

$$P = F V_2 \qquad \dots\dots\dots(7)$$

---

[x] This expression for power output is only true when the drag on the blades and the losses in the slipstream are neglected.

and the power coefficient C_P in terms of the windmill swept area πR_t^2 and the upstream velocity V_o is

$$C_P = \frac{P}{\frac{1}{2}\rho\pi R_t^2 V_o^3} \qquad \ldots\ldots\ldots\ldots(8)$$

If $S_2 = \pi R_t^2$ then from equations (3), (7) and (8)

$$C_P = f\,v^3 \qquad \ldots\ldots\ldots\ldots(9)$$

and from equation (5)

$$C_P = f\,v^3 = (h_1 v - h_2\,v^3) \qquad \ldots\ldots\ldots\ldots(9a)$$

If the internal duct friction is neglected $\triangle H_1 = \triangle H_2 = \triangle H_3 = 0$ then the power coefficient can be written $C_{P_{ideal}}$, where

$$C_{P_{ideal}} = \left[\left(1 - C_{p_4}\right) - \mu^2 v^2\right]v \qquad \ldots\ldots\ldots\ldots(10)$$

which equals the power coefficient obtained from equation (21) in the previous section.

Both equations (9a) and (10) show very clearly that large power coefficients will be obtained when C_{p_4} is negative, μ is very small and v is very large, although these variables are not independent.

For fixed values of h_1 and h_2 the maximum power coefficient is obtained when

$$v = \sqrt{\frac{h_1}{3\,h_2}} \qquad \ldots\ldots\ldots\ldots(11)$$

giving

$$\left.\begin{array}{l} C_{P_{max}} = 2\,h_2\left(\dfrac{h_1}{3\,h_2}\right)^{3/2} \\[3mm] \left(C_{P_{ideal}}\right)_{max} = \dfrac{2}{3^{3/2}}\,\dfrac{\left(1 - C_{p_4}\right)^{3/2}}{\mu} \end{array}\right\} \qquad \ldots\ldots\ldots\ldots(12)$$

and
$$f_{\text{at } C_{P_{max}}} = 2 h_2$$

$$\left(f_{ideal}\right)_{\text{at } C_{P_{max}}} = 2 \mu^2$$

...............(13)

It can be seen that the entry contraction ratio S_1/S_2 only affects the performance insofar as it affects the losses $\triangle H_1$ and $\triangle H_2$ and the pressure coefficient C_{p_4}. The factors of greatest importance are the expansion ratio of the diffuser, $\frac{1}{\mu}$, the diffuser loss, $\triangle H_3$, and the pressure coefficient, C_{p_4}.

A measure of the gain in power output from the ducted windmill over the unshrouded windmill is the ratio of their respective power coefficients. Thus if both windmills have the same swept area, πR_t^2, and the unshrouded windmill is operating at its maximum output power coefficient C_P' then the performance factor r is given by

$$r = \frac{C_P}{C_P'} = \frac{27}{16} f v^3 \qquad \text{...............(14)}$$

When in addition the ducted windmill is operating under maximum power conditions we find from equation (12) that

$$\frac{C_{P_{max}}}{C_P'} = \left(\frac{3 h_1}{4}\right)^{3/2} \Big/ h_2^{\frac{1}{2}} \qquad \text{............(15)}$$

or using the values of h_1 and h_2

$$\frac{C_{P_{max}}}{C_P'} = \left[\frac{\left\{ \frac{3}{4}\left(1 - C_{p4} - \frac{\triangle H_1}{\frac{1}{2}\rho V_0^2}\right)\right\}^3}{\left(\mu^2 + \frac{\triangle H_2}{\frac{1}{2}\rho V_2^2} + \frac{\triangle H_3}{\frac{1}{2}\rho V_3^2}\right)} \right]^{\frac{1}{2}} \qquad \text{............(15a)}$$

and
$$\frac{\left(C_{P_{ideal}}\right)_{max}}{C_P'} = \frac{1}{\mu} \left[\frac{3\left(1 - C_{p4}\right)}{4} \right]^{3/2} \qquad \text{............(16)}$$

The limit of usefulness of the ducted windmill can be taken when C_P/C_P' equals unity. Thus with no internal losses and $C_{p_4} = 0$ the minimum value of the expansion ratio $\frac{1}{\mu}$, corresponding to $\left(C_{P_{ideal}}\right)_{max}/C_P'$, is, from equation (16)

$$\frac{1}{\mu} = 1.54 \qquad \ldots\ldots\ldots\ldots(17)$$

In addition, from equation (13), it can be shown that the corresponding maximum value of the disc loading is

$$\left(f_{ideal}\right)_{at\ C_{P_{max}}} = 0.84 \qquad \ldots\ldots\ldots\ldots(18)$$

These results show, when internal duct losses are neglected, that the ducted windmill has a greater output than the unshrouded windmill when the external pressure coefficient, C_{p_4}, is negative or zero, and the expansion ratio of the diffuser, $\frac{1}{\mu}$, is greater than 1.54. Also the disc loading is reduced from 2 to less than 0.84 when the windmill is operating under maximum power conditions. Thus when internal losses are neglected, the gain in power, with the ducted windmill, is proportional to the diffuser expansion ratio and similarly the disc loading is inversely proportional to the square of the diffuser expansion ratio.

(iii) Tip clearance of the ducted windmill

Since the action of a windmill is to create a pressure drop across it, similar to the action of a gauze, it is important to consider what effect the clearance between the blades and the duct has on the reduction of mass flow through the windmill and the power output.

Assume that the windmill of disc area S is uniformly loaded and is placed in a duct of area S_2 (figure 5). The velocity and pressure are respectively V_o, p_o far upstream and V_3, p_2 far downstream in the slipstream and V_2, p_2 outside. Frictional losses will be neglected throughout. If we apply Bernoulli's equation to the flow inside and outside the slipstream then

$$H_o = p_o + \tfrac{1}{2}\rho V_o^2 = p_2 + \tfrac{1}{2}\rho V_2^2 \qquad \ldots\ldots\ldots\ldots(1)$$

and $\quad H_1 = p_2 + \frac{1}{2}\rho V_3^2$

where H_0 is the total head upstream of the windmill and outside the slipstream and H_1 is the total head downstream of the windmill.

If Δp is the uniform pressure drop across the windmill then

$$\Delta p = H_0 - H_1 = \frac{1}{2}\rho \ (V_2^2 - V_3^2) \qquad \dots\dots\dots\dots(2)$$

and the axial force, F, on the windmill is given by

$$F = \Delta p \ S \qquad \dots\dots\dots\dots(3)$$

If we apply the momentum theorem to the control surface ABCD (figure 5) then it can be shown that

$$F = \frac{\rho}{2} \ S_2 \ (V_0^2 - V_2^2) + \rho S_3 \ (V_2^2 - V_3^2) \qquad \dots\dots\dots\dots(4)$$

From continuity it follows that

$$S_2 V_0 - S_3 V_3 = (S_2 - S_3)V_2 \qquad \dots\dots\dots\dots(5)$$

giving $\quad \dfrac{S_3}{S_2} = \dfrac{V_2 - V_0}{V_2 - V_3} \qquad \dots\dots\dots\dots(6)$

If $\dfrac{\Delta p}{\frac{1}{2}\rho V_0^2} = k$ then equations (2) and (4) can be

written respectively

$$V_2^2 = V_3^2 + k \ V_0^2 \qquad \dots\dots\dots\dots(7)$$

and $\quad \dfrac{V_3^2}{V_0^2} = 1 - k \ \left(\dfrac{S}{S_2} + 1 - 2 \ \dfrac{S_3}{S_2} \right) \qquad \dots\dots\dots\dots(8)$

From equation (6), (7) and (8) we obtain

$$\frac{V_2 - V_o}{V_2 - V_3} = \frac{1 - \left(\frac{V_o}{V_3}\right)^2 \left(1 - k\left(1 + \frac{S}{S_2}\right)\right)}{2k\left(\frac{V_o}{V_3}\right)^2} \qquad \ldots\ldots\ldots(9)$$

If we put $n = \frac{S}{S_2}$; $x = \frac{V_2}{V_3}$; $z = \frac{V_o}{V_3}$ then equations (7) and (9) become

$$x^2 = 1 + k z^2 \qquad \ldots\ldots\ldots\ldots(10)$$

and $\left(\frac{x - z}{x - 1}\right) = \frac{1 - z^2(1 - k - kn)}{2kz^2} \qquad \ldots\ldots\ldots\ldots(11)$

On elimination of x between equations (10) and (11) we obtain for z

$$a z^4 + b z^3 + c z^2 + d z + e = 0 \qquad \ldots\ldots\ldots\ldots(12)$$

where $\quad a = -\left[k^2(1-n)^2 - 2k(1+n) + 1\right]$; $d = -4$
$\qquad b = 4\left[1 - k(1+n)\right] \qquad\qquad$; $e = 3$
$\qquad c = 2k(1+n) - 2$

When the value of $\frac{S}{S_2}$ is near unity the solution of equation (2) is

$$z = \frac{V_o}{V_3} = 1 + \frac{k(1-n)}{2\sqrt{1+k}} \qquad \ldots\ldots\ldots\ldots(13)$$

and $x = \frac{V_2}{V_3}$ can be found from equation (10).

If V is the mean axial velocity through the windmill disc the power output, P, is equal to

$$P = FV \qquad \ldots\ldots\ldots\ldots(14)$$

where $\quad V = V_3 \left(\frac{V_2 - V_o}{V_2 - V_3}\right) \frac{S_2}{S}$

When the value of $\frac{S}{S_2}$ is near unity the power output coefficient, using equation (13) for z, is

$$C_P = \frac{P}{\frac{1}{2}\rho V_o^3 S_2} = kn\frac{V}{V_o} = \frac{k}{z}\left(\frac{x-z}{x-1}\right) = k\left(1 - \frac{(1-n)k}{2\left\{\sqrt{1+k}-1\right\}}\right) \quad (15)$$

For an ideal windmill i.e. one having no tip clearance, $n=1$ and $C_{P_{ideal}} = k$. Thus the loss in power due to tip clearance expressed as a ratio is

$$\frac{C_P}{C_{P_{ideal}}} \approx 1 - \frac{(1-n)k}{2\left\{\sqrt{1+k}-1\right\}} \quad \dots\dots\dots\dots(16)$$

For moderate tip clearances the loss in power is less than 1 per cent and hence the neglect of tip clearance in the previous calculations is justified.

4c. Calculated results and discussion

The optimum performance of ducted windmills having diffuser expansion ratios, $1/\mu$, of 2,3,4 and 5 and internal total head loss coefficients of 0, 0.10, 0.15, 0.20 and 0.25 have been computed for values of duct exit pressure coefficient C_{p_4} of 0, -0.1, -0.2 and -0.3. The entry loss coefficient $\frac{\Delta H_1}{\frac{1}{2}\rho V_o^2}$ has been made zero throughout, since this will be its value in nearly all well designed duct systems. These results shown in tables 1,2,3 and 4 have been compared with the optimum performance of an unshrouded windmill. The results are plotted in figures 6,7,8,9 and 10.

Inspection of figures 6,7,8,9,10 shows that the performance factor r depends critically on the value of the pressure coefficient, C_{p_4}, at exit. Thus the power output of a ducted windmill will be increased significantly if the diffuser outlet is placed in the lee of an obstacle or by providing a flow augmentor as shown in figure 1.

If we assume that a duct of good aerodynamic design

has an internal loss coefficient of 0.15, then with $C_{p_4} = -0.15$

and a diffuser expansion ratio of 3.5, figure 8 shows that the ducted windmill gives an output power 65 per cent greater than that of the ideal unshrouded windmill. If the diffuser expansion ratio is increased to 5.0 the gain in the output power would reach 85 per cent but it is questionable whether the increased cost of the longer duct would justify this gain in performance.

Another important advantage of the ducted windmill over the unshrouded windmill is the reduction in disc loading. This is clearly seen on inspection of tables 1b and 1c. For instance with a diffuser expansion ratio of 3.5 the disc loading of the ducted windmill is only 25 per cent of that of the free windmill case. This effect will considerably simplify the design of the ducted windmill and will result in a reduction of the blade cost which will partly offset the cost of the ducting. It is interesting to note that the Reynolds number, based on the windmill chord, will be of similar order in the two cases, since although the axial velocity will be increased, the blade chord can be reduced due to the smaller disc loading of the ducted windmill.

In addition to the reduction in disc loading the gust loads on the blades of the ducted windmill will be much smaller than for the unshrouded windmill. This is because the contraction cone ahead of the windmill will tend to improve the uniformity of flow across the windmill and to reduce any unsteadiness in the flow. In order to take maximum advantage of this effect, the contraction ratio should be at least 1.5.

PART II

5. The generalised momentum theory of windmills

5a. The unshrouded windmill

In the one-dimensional or simple momentum theory discussed in paragraph 4 the effect of the finite number of blades has been neglected, and it has been assumed that the induced velocity in the windmill slipstream is axial and uniform over any normal cross-section of the slipstream. In the generalised momentum theory, both the axial and rotational components of the induced velocity, arising from the vortex sheets shed from each of the windmill blades, are included as well as their variation over the slipstream and with time. The calculation of the induced velocities will be left to the section below on the vortex theory of windmills but in the present paragraph expressions will be obtained for the mean values of axial (drag) force and power output in terms of the mean axial velocity far downstream of the windmill. Although the major effects of the finite number of blades are included their drag is neglected.

If we assume that our windmill is designed to have a minimum energy loss it follows from the work of Betz that the vortex sheets shed from each blade move backwards as solid helicoidal screw surfaces having constant pitch. Far downstream of the windmill these vortex sheets will be of a constant diameter, greater than that of the windmill owing to the slipstream expansion.

The laws of conservation of mass, momentum and energy will be applied to the control surface ABCD (see figure 11) in order to find the mean axial force, torque, and power output from the windmill. An element of the surface AD, far upstream, will be denoted by dS_o where the velocity and pressure are V_o and p_o respectively. Similarly, far downstream, the element of the surface BC will be denoted by dS_∞ where the axial component of the velocity and pressure are u_1 and p_1 respectively. The windmill, which is rotating with an angular velocity Ω, has B blades which are equispaced and straight. It is assumed to have no hub, fairings or guide vanes. The axial force on the windmill is F and the axial force, due to the pressure of the external flow on the curved boundaries of the slipstream, will be denoted by X.

If we therefore equate the rates of flow of momentum across the control surface ABCD with the pressure forces on the boundary and the internal body forces we can show that (see figure 11)

$$F = X + p_o(S_o - S_\infty) + \oint (p_o - p_1 + \rho u_1 V_o - \rho u_1^2)dS_\infty$$

$$\ldots\ldots\ldots\ldots(1)$$

But from an analysis of the flow outside the windmill slip-stream it can be shown that

$$X = p_o (S_\infty - S_o) \qquad\ldots\ldots\ldots\ldots(2)$$

giving

$$F = \oint (p_o - p_1 + \rho u_1 V_o - \rho u_1^2) \, dS_\infty \ldots\ldots\ldots\ldots(3)$$

Since we are assuming that the vortex sheets are moving through the fluid as solid helicoidal surfaces the induced motion, far downstream, can be derived in terms of the velocity potential $\emptyset$ (div $\emptyset$ = $\underset{\sim}{q}$) satisfying the boundary conditions of no flow across the vortex sheets and no flow, relative to the sheets, at infinity. Hence $(p_o - p_1)$ can be found in terms of the induced velocity components from Bernoulli's equation for the unsteady flow of an incompressible fluid. Thus

$$p_o - p_1 = \frac{\rho}{\partial t}\frac{\partial\emptyset}{} + \frac{\rho q_1^2}{2} \qquad\ldots\ldots\ldots\ldots(4)$$

where $\emptyset$ is the velocity potential at a point r, θ, z (cylindrical polar coordinates) due to the axial movement of the solid helicoidal surfaces through the fluid with the velocity w_o , and p_o is the pressure in the fluid at infinity. Now because the vortex sheets are moving with the velocity w_o in the direction of the negative z-axis it can be shown that

$$\emptyset = \emptyset (z + w_o t, r, \theta) \qquad\ldots\ldots\ldots\ldots(5)$$

If $\qquad u_r = \frac{\partial\emptyset}{\partial r}$; $u_\theta = \frac{1}{r}\frac{\partial\emptyset}{\partial\theta}$; $u_z = \frac{\partial\emptyset}{\partial z}$ then equation

(4) becomes, following Theordorsen[11],

$$p_o - p_1 = \rho w_o u_z + \frac{\rho q_1^2}{2} \qquad\ldots\ldots\ldots\ldots(6)$$

where $q_1^2 = u_r^2 + u_\theta^2 + u_z^2$

and equation (3) becomes, since $u_1 = V_o + u_z$,

$$F = \rho \oint \left[\frac{q_1^2}{2} - u_z^2 - u_z (V_o - w_o) \right] d S_\infty \quad \ldots (7)$$

Since q_1 is a function of time we must integrate equation (7) with respect to time in order to find the mean value of the axial force. But since ϕ is a function of $z + w_o t$ an integration with respect to t may be replaced by an integration with respect to z. The resultant volume integral can be taken over an infinite cross-section normal to the z axis and a distance along the z-axis equal to the distance between successive vortex sheets. This distance is equal to H/B where H is the pitch of each vortex sheet and B is the number of blades. Hence the mean value of the axial (drag) force is

$$F = \frac{\rho B}{H} \iiint \left[\frac{q_1^2}{2} - u_z^2 - u_z (V_o - w_o) \right] dv \quad \ldots (8)$$

where dv is the element of volume.

Now Theordorsen has shown that the separate integrals on the right hand side of equation (8) can be written in terms of the integral of the circulation taken over the vortex sheets in the slipstream of radius R_∞. If the circulation at radius r is denoted by $\Gamma(x)$ where $x = r/R_\infty$ and

$$\Gamma(x) = \frac{w_o H K(x)}{B} \qquad \text{then we can write}$$

$$\begin{aligned}
\frac{B}{H} \int u_z \, dv &= - w_o \, k \, \pi \, R_\infty^2 \\[2mm]
\frac{B}{H} \int q_1^2 \, dv &= w_o^2 \, k \, \pi \, R_\infty^2 \\[2mm]
\frac{B}{H} \int u_z^2 \, dv &= w_o^2 \, e \, \pi \, R_\infty^2
\end{aligned} \right\} \quad \ldots (9)$$

where $k = 2 \int K(x) \, x \, dx$.

If we substitute equations (9) into (8) then

$$\frac{F}{\frac{1}{2}\rho V_o^2 \pi R_t^2} = C_F = 2k\,\bar{w}_o \left[1 - \bar{w}_o \left(\frac{1}{2} + \frac{e}{k}\right)\right] \frac{R_\infty^2}{R_t^2} \quad \ldots\ldots\ldots(10)$$

where $\bar{w}_o = w_o/V_o$.

Similarly it can be shown that the mean energy loss, E, in the windmill slipstream can be written

$$C_E = \frac{E}{\frac{1}{2}\rho V_o^2 \pi R_t^2} = 2k\,\bar{w}_o^2 \left(\frac{1}{2} - \frac{e}{k}\,\bar{w}_o\right) \frac{R_\infty^2}{R_t^2} \quad \ldots\ldots\ldots(11)$$

But the power output, P, is equal to $\Omega Q = (FV_o - E)$, where Q is the output torque and Ω is the angular velocity of the windmill. Hence the power coefficient C_P is given by

$$C_P = \frac{P}{\frac{1}{2}\rho V_o^3 \pi R_t^2} = 2k\,\bar{w}_o (1-\bar{w}_o) \left(1 - \frac{e}{k}\,\bar{w}_o\right) \frac{R_\infty^2}{R_t^2} \quad \ldots\ldots(12)$$

Equations (10) to (12) can be compared with the corresponding expressions obtained from the one-dimensional theory. These are, if $S_2 = \pi R_t^2$, and $V_\infty = V_o - w_o$ (see section 4a)

$$\left.\begin{array}{l} C_F = 2\bar{w}_o \left(1 - \dfrac{\bar{w}_o}{2}\right) \\[2ex] C_E = \bar{w}_o^2 \left(1 - \dfrac{\bar{w}_o}{2}\right) \\[2ex] C_P = 2\bar{w}_o \left(1 - \dfrac{\bar{w}_o}{2}\right)^2 \end{array}\right\} \quad \ldots\ldots\ldots(13)$$

and they are similar to the previous equations when
$$\frac{R_\infty^2}{R_t^2} = \frac{1 - \bar{w}_o/2}{1 - \bar{w}_o} \quad,\quad k = 1 \quad \text{and} \quad e/k = \frac{1}{2}.$$ For an infinite number of blades when $\dfrac{V_o - w_o}{\Omega R_\infty}$ is small $k = e = 1$ and therefore since $e/k = \frac{1}{2}$ is not the limiting value we cannot expect that the optimum performance, found from the simple theory, will be equal to that found from the more exact theory.

Theordorsen calls k the mass coefficient, and

interprets it as the ratio of the mean rearward velocity, taken over the entire slipstream cross-section, to the rearward velocity w_o. Both k and e are functions of B and $\frac{V_o - w_o}{\Omega R_\infty}$ and their values can be obtained from the tables given in reference 11.

Before equations (10) to (12) can be used to predict the performance of a windmill the slipstream expansion must be found. From the simple theory we find that

$$\frac{R_\infty^2}{R_t^2} = \frac{1 - \bar{w}_o/2}{1 - \bar{w}_o} \qquad\qquad \dots\dots\dots\dots(14)$$

$$\approx 1 + \bar{w}_o/2 \quad \text{for small } \bar{w}_o .$$

A better approximation is due to Theordorsen who shows that from first order calculations of the radial velocities in the slipstream,

$$\frac{R_\infty^2}{R_t^2} = \frac{\left(1 - \bar{w}_o\right)\left(1 - \frac{\bar{w}_o}{2} s\right)}{\left(1 - \bar{w}_o/2\right)\left(1 - \bar{w}_o\left(\frac{1}{2} + \frac{e}{k}\right)\right)} \qquad \dots\dots\dots\dots(15)$$

$$\approx 1 + \bar{w}_o\left(\frac{e}{k} - s/2\right) \quad \text{for small } \bar{w}_o$$

where $\quad s = \dfrac{\displaystyle\int_0^1 x\,K(x)\cos^2\emptyset\,dx}{\displaystyle\int_0^1 x\,K(x)\,dx} \quad$ is the average value of

$\cos^2\emptyset$ weighted by the factor $x\,K(x)$,

and $\quad \emptyset = \tan^{-1}\left[\dfrac{V_o}{\Omega R_o}\dfrac{(1 - \bar{w}_o/2)}{x}\right] \quad$ is the angle of

the relative flow at the windmill. When $\dfrac{V_o - w_o}{\Omega R_\infty}$ is small

$\left(\dfrac{e}{k} - \dfrac{s}{2}\right) \approx 0.5$, and $s \approx 1.0$, and then equations (14) and (15)

become equal, at least for small values of $\bar{w}_o$. For approximate

calculations s can be put equal to the mean value of $\cos^2\phi$ over the wake (i.e. approximately the value of $\cos^2\phi$ at $x^2 = 0.50$) or

$$s \approx \frac{1}{1 + \frac{2}{\mu_o^2}\left(1 - \frac{\bar{w}_o}{2}\right)^2} \qquad \dots\dots\dots\dots(16)$$

where $\mu_o = \dfrac{\Omega R_t}{V_o}$.

Since the power output, P, is a function of the number of blades, B, the ratio of the peripheral speed to the wind velocity, μ_o, and $\bar{w}_o$ no simple relation, in general, exists for its maximum value. However when $V_o/\Omega R_t$ is very small k and e have values near unity and if we use the approximate value of the slipstream expansion ratio (equation (14)) then it can be shown that the maximum power output occurs when

$$\left.\begin{array}{lll} & \bar{w}_o & = 0.422 \\[2mm] \text{giving} & C_{P_{max}} & = 0.385 \\[2mm] \text{and} & C_F & = 0.424 \\[2mm] & (\text{at } C_{P_{max}}) \end{array}\right\} \qquad \dots\dots\dots\dots(17)$$

The corresponding values obtained from the simple theory are,

$$\left.\begin{array}{ll} \bar{w}_o & = 2/3 \\[2mm] C_{P_{max}} & = 16/27 = 0.593 \\[2mm] C_F & = 8/9 \\[2mm] \text{at } C_{P_{max}} \end{array}\right\} \qquad \dots\dots\dots\dots(18)$$

However when we use the more correct expression for R_∞^2/R_t^2 from equation (15) we see that R_∞/R_t tends to infinity when $\bar{w}_o = \dfrac{1}{\left(\frac{1}{2} + e/k\right)}$ (i.e. when μ_o is large $\bar{w}_o = 2/3$). The power coefficient C_P does not reach a maximum for a value of

$\bar{w}_o \leqslant 2/3$, when equation (15) is used for $\left(\dfrac{R_\infty}{R_t}\right)^2$ in equation (12), but tends to infinity with R_∞/R_t. It appears therefore that equation (15) is not satisfactory when the slip-stream expansion is large and it must be expected that the calculation of the radial velocities according to a second order theory would lead to a modified formula for R_∞/R_t. In practice an instability must arise for some value of $\bar{w}_o$ less than unity. In view of this instability in the operation of the windmill the values of $\bar{w}_o$ and $C_{P_{max}}$ given by equation (17) may more nearly represent the limiting conditions obtainable in practice.

So far we have found the maximum power conditions in terms of $\bar{w}_o$ but it is more important to state how the power output depends on the ratio $\Omega R_t/V_o$ for a given fixed pitch windmill. If we consider the blade lift loading at a radius of $0.75 R_t$, say, as representative of the overall blade loading we can relate $\bar{w}_o$ to μ_o and θ, the blade angle at this radius. From the vortex theory of windmills the following relation exists, for the ideal windmill, between the local blade angle, θ, and the local lift loading [11]

$$\sigma \, C_L = \frac{2K(x) \, \bar{w}_o \, (1 - \bar{w}_o)}{\left(1 - \bar{w}_o/2\right)\left(1 - \dfrac{\bar{w}_o}{2} \cos^2\phi\right)} \; \frac{\sin^2\phi}{\cos\phi} \qquad \ldots\ldots(19)$$

where $\quad \theta \;=\; \phi - a$

$$C_L \;=\; a_o(\phi - \theta - a_o)$$

and $\quad \tan\phi \;=\; \dfrac{V_o \, (1-\bar{w}_o/2)}{\Omega R_t \, x}$

ϕ is the angle of relative flow, a is the angle of incidence, a_o is the blade no-lift angle, a_o is the lift curve slope and σ is the blade solidity. If suitable values are chosen for σ, a_o, μ_o and a_o it can be shown from equation (19) that the blade incidence, a, increases from its no-lift value at $\bar{w}_o = 0$ to its maximum value at about $\bar{w}_o = 0.42$ and falls again

to its no-lift angle when $\bar{w}_o = 1.0$. This indicates that the approximate relation for the slipstream expansion given by equation (14), which leads to a maximum power output coefficient, C_P, at $\bar{w}_o = 0.42$, may be more representative than equation (15) for large values of $\bar{w}_o$.

For small values of $V_o/\Omega R_t$, $K(x)$ at $x = 0.75$ is approximately equal to unity. If further we assume that $\tan\emptyset = \sin\emptyset = \emptyset$ and $\cos\emptyset = 1$ then, from equation (19), we find after some rearrangement that

$$\bar{w}_o^2 - \bar{w}_o\, P_1 + P_2 = 0 \qquad \dots\dots\dots\dots(20)$$

where $\qquad P_1 = 1 + \dfrac{3}{16}\mu_o\,(\sigma\,a_o)_{0.75}$

and $\qquad P_2 = \dfrac{3}{8}\mu_o\,(\sigma\,a_o)_{0.75}\left[1 - \dfrac{3\mu_o}{4}(\theta + a_o)_{0.75}\right]$

Real values of $\bar{w}_o$ can only be obtained from equation (20) when

$$\theta_{0.75} \geqslant \frac{\left[\dfrac{9}{8}\mu_o\,(\sigma\,a_o)_{0.75} - 1\right]}{\dfrac{9}{8}\mu_o^2\,(\sigma\,a_o)_{0.75}} - \left(a_o + \dfrac{\sigma\,a_o}{32}\right)_{0.75} \quad (21)$$

For both small and large $\emptyset$ equation (19) shows that $C_L = 0$ when $\bar{w}_o = 1$. It follows, from equation (19), that for values of $\bar{w}_o \leqslant 1$

$$\theta_{0.75} \geqslant \tan^{-1}\left(\frac{2}{3\mu_o}\right) - a_o \qquad \dots\dots\dots\dots(22)$$

a relation which is independent of the blade solidity. Equations (21) and (22) represent the onset of instability and correspond to the critical values of $\bar{w}_o$ noted above.

At the other end of the range zero power output is obtained when $\bar{w}_o = 0$. This occurs when

$$\mu_o = \frac{4}{3}\cot(\theta + a_o)_{0.75} \qquad \dots\dots\dots\dots(23)$$

When $\mu_o = 0$ equation (23) shows that the maximum value of θ

is given by

$$(\theta^{o}_{max})_{0.75} = 90^{o} - a^{o}_{o} \qquad \cdots\cdots\cdots\cdots(24)$$

The limits imposed on $\tilde{w}_o$ and θ above, for large values of $\bar{w}_o$, correspond very closely to the limit of stable operation observed experimentally by Iwasaki[4] for windmills of less than 4 blades having values of θ less than 20°.

It should be noted that in the determination of the above results the drag on the blades has been neglected. It is therefore probable that for large values of $\bar{w}_o$ some of these relations will need modification. In order to find the reduction in power output due to the energy lost in overcoming the (profile) drag of the blades we must add to the energy loss E the amount E_D where

$$\frac{E_D}{\frac{1}{2}\rho V_o^3 (\pi R_t^2)} = \frac{1}{\pi R_t^2} \int_o^{R_t} Bc \, C_D \left(\frac{W}{V_o}\right)^3 \, dr \quad \cdots\cdots\cdots\cdots(25)$$

where c is the blade chord

           W is the resultant velocity

           C_D is profile drag coefficient.

Since the resultant velocity,

$$W = \frac{V_o \left(1 - \frac{\bar{w}_o}{2} \cos^2\phi\right)}{\sin\phi} \quad \text{(see section 6) and the}$$

lift coefficient, C_L, can be found from equation (19) we can rewrite (25) as follows

$$\frac{E_D}{\frac{1}{2}\rho V_o^3 (\pi R_t^2)} = \frac{2 \bar{w}_o (1-\bar{w}_o) k \, \triangle}{\mu_o} \quad \cdots\cdots\cdots\cdots(26)$$

where $\triangle = \dfrac{\displaystyle\int_o^1 x \, K(x) \left(\dfrac{C_D \bar{W}^2}{C_L \, x}\right) dx}{\displaystyle\int_o^1 x \, K(x) \, dx}$

and $\bar{W} = W/V_o$.

The power coefficient corrected for blade profile drag becomes

$$C_P = 2k\,\bar{w}_o\,(1-\bar{w}_o)\left[\left(\frac{R_{\infty}}{R_t}\right)^2 \left(1 - \frac{e}{k}\,\bar{w}_o\right) - \frac{\Delta}{\mu_o}\right] \quad\text{.......(27)}$$

Since Δ is the average value of $(C_D\bar{W}^2/C_L\,x)$ weighted by the factor $x\,K(x)$ we can find an approximate value for it by putting it equal to its value at $x^2 = 0.50$, or

$$\frac{\Delta}{\mu_o} \approx \frac{\sqrt{2}}{\mu_o}\left(\overline{\frac{C_D}{C_L}}\right)\frac{\left(\frac{\mu_o^2}{2} + 1 - \frac{\bar{w}_o}{2}\right)^2}{\frac{\mu_o^2}{2} + \left(1 - \frac{\bar{w}_o}{2}\right)^2} \quad\text{............(28)}$$

where $\overline{\dfrac{C_D}{C_L}}$ is the value of $\dfrac{C_D}{C_L}$ at $x = \dfrac{1}{\sqrt{2}}$.

If finally we substitute for $\dfrac{R_{\infty}}{R_t}$ from equation (14) then for values of $\bar{w}_o$ below about 0.75, and large μ_o,

$$C_P = 2k\,\bar{w}_o\left(1 - \frac{\bar{w}_o}{2}\right)\left(1 - \frac{e}{k}\,\bar{w}_o\right)\left[1 - \frac{(1-\bar{w}_o)}{\left(1 - \frac{\bar{w}_o}{2}\right)}\frac{\overline{\frac{C_D}{C_L}}\,(2+\mu_o^2)}{\sqrt{2}\,\mu_o\left(1 - \frac{e}{k}\,\bar{w}_o\right)}\right]$$

$$\text{............(29)}$$

It follows that for normal values of C_D/C_L, say about 40, the drag correction to the power coefficient for moderate disc loadings is less than 5 per cent and it changes the value of $\bar{w}_o$, corresponding to maximum power coefficient, by less than 2 per cent.

Although these results have been obtained for an unshrouded windmill it will be shown below that very similar relations also exist for the ducted windmill.

5b. The ducted windmill

(i) Discussion

In section (4) above the performance of the ducted windmill has been obtained on the assumption that the flow is one-dimensional throughout and the number of blades is infinite. Although in section (4b) the frictional losses in the duct have been included no account was taken of the energy losses in the slipstream due to the rearward movement of the helical vortex sheets shed from each blade of the windmill. In addition although the interdependence of the windmill and its fairing were noted and allowed for approximately no attempt was made to determine a correct formulation of the problem.

Let us assume in this section that we are considering the performance of an ideal windmill, that is one in which the vortex sheets shed from the blades move rearward far downstream as solid helicoidal surfaces, mounted in a duct of arbitrary cross-section. It is then possible to calculate the axial force, energy loss and power output in terms of w_o , the axial displacement velocity of the vortex sheets far downstream, and the fairing (or duct) drag.

(ii) Flow through the duct

If we neglect the rotational effects in the windmill slipstream and assume that the axial velocity far downstream is uniform over the slipstream, then it is permissible to replace the windmill by a gauze, having a pressure drop equal to that created by the windmill (figure 12).

The calculation of the internal and external pressure distribution over the duct alone in an inviscid flow can be performed by the method of singularities in which the duct is replaced by a suitable distribution and strength of sources, sinks and vortices. Alternatively for a given distribution of singularities, or prescribed internal and external velocity distributions the shape of the duct can be calculated.

When the gauze is present in the duct the method of calculation is similar but is complicated by the vortex sheet boundary downstream of the duct exit between the slipstream and the free stream. The flow inside the slipstream is at a lower total head than the flow outside but the pressure across the vortex sheet is constant. A discontinuity must therefore arise in the tangential velocities on each side of the vortex sheet. The main difficulty in the calculation is that the shape and strength of the vortex sheets are not known initially but can only be determined when the calculation is complete.

The standard method of calculation is to replace the vortex sheet by a solid boundary across which a pressure drop acts, equal to that across the gauze. The gauze is then removed and the complete flow, internal and external, is then homogenous since the flow is at constant total head everywhere. The shape of the vortex sheet and the velocity distribution around the complete duct can be found by an iterative method.[15] Finally the velocity distribution across the plane of the windmill can be determined.

The viscous effects on the pressure distribution around the duct can be determined from a calculation of the boundary layer displacement thickness using the first approximation to the pressure distribution. The above calculation for the pressure distribution must then be repeated for the new 'effective' duct shape. Thus finally the duct drag can be determined as a sum of the tangential stress and normal pressure components together with the velocity distribution across the plane of the windmill.

Naturally in some cases it would be better to find the drag of the duct, housing the gauze, experimentally, although in all cases the theoretical calculations will show clearly what shape of duct is necessary to avoid separation of the boundary layer especially close to the duct exit.＊ It should be noted that very little experimental information is available on the performance of ducted intakes of the type required for the ducted windmill. It is therefore important that a combined theoretical and experimental programme should be drawn up to investigate the most suitable external and internal profiles to suit the performance of high efficiency ducted windmills.

(iii) Performance of the ducted windmill

It will be assumed that the neglect of the rotational components of the velocity in the slipstream in calculating the drag and velocity distribution in the plane of the windmill produces negligible errors in the values of these quantities.

＊ It can be readily shown, according to inviscid flow theory, that for ducts having a finite trailing edge angle a stagnation point of the internal flow, but not of the external flow, must exist at the trailing edge in order to satisfy the condition of constant pressure across the vortex sheet springing from the trailing edge. In consequence there will exist, close to the duct exit, a region of large positive pressure gradient which, in the real flow, might tend to cause separation of the internal flow.

It will be assumed also that the velocity distribution
through the windmill disc is equal to the sum of the slip-
stream and duct effects calculated separately. The value
of the duct velocity obtained in section (ii) is based on
the slipstream velocity being uniform. Thus if $V_2(x)$ is
the velocity in the plane of the windmill, when the uniform
velocities in the slipstream are V_0 and V_{∞}, respectively,
far upstream and downstream then the contribution to V_2 due
to the duct is

$$\delta V_2(x) = V_2(x) - \left(\frac{V_0 + V_{\infty}}{2}\right).$$ The additional

contribution to $V_2(x)$ due to the motion of the helicoidal
vortex sheets inside the duct vortex sheets far downstream
of the duct exit will be discussed below.

The axial force on a ducted windmill, in which the
effects of friction are included, can be found from an
application of the momentum equation to the three regions
shown in figure 13.

Let BCD and BFE represent the displacement of
the boundaries of the duct and its wake to allow for the
effects of the boundary layer.

In region I outside the duct

$$p_0 (S'_{\infty} - S_0) - \int_{A-B-C-D} p \, dS = 0 \qquad \dots\dots\dots\dots(1)$$

In region II the total drag force on the duct,
including friction is

$$D = -p_0(S'_{\infty} - S_{\infty}) + \int_{BD-BE} p \, dS + \rho \int_{wake} u(V_0 - u) dS \quad \dots\dots\dots(2)$$

In region III the axial force on the windmill is

$$F = p_0(S_0 - S_{\infty}) + \int \left[(p_0 - p_1) + \rho u_1(V_0 - u_1) \right] dS_{\infty} + \int_{A-B-F-E} p \, dS$$
$$\dots\dots\dots\dots(3)$$

Thus from (1) and (3)

$$F = \int \left[\bar{p}_0 - p_1 + \rho u_1 (V_0 - u_1) \right] d\, S_\infty + \int_{BE-BD} p\, dS + p_0 (S'_\infty - S_\infty) \qquad \dots\dots\dots\dots(4)$$

and from (2) and (4)

$$F+D' = \int \left[\bar{p}_0 - p_1 + \rho u_1 (V_0 - u_1) \right] d\, S_\infty \qquad \dots\dots\dots\dots(5)$$

where

$$D' = D - \rho \int_{wake} u(V_0 - u)\, dS = \int_{BD-BE} p\, dS - p_0 (S'_\infty - S_\infty)$$

The duct drag force can be calculated, as explained above, by replacing the vortex sheet FE by a solid boundary when the windmill is removed. It is assumed that the pressure drop, Δp, across the windmill is uniform across the plane of the windmill. Thus when the windmill is removed the vortex sheets CD and EF can only be similarly placed when a pressure difference Δp is applied across them. Since the flow inside and outside the duct is then homogenous, the velocity and pressure distribution inside and outside the duct boundaries can be calculated. Allowance can be made for boundary layer effects and in particular their effect on the duct pressure distribution and the effective duct area, S_∞, far downstream. The duct drag can then be obtained.

The integral on the right hand side of equation (5) is identical with that for the unshrouded windmill, if we assume that far downstream of the windmill the vortex sheets are moving as rigid surfaces. Therefore from equation (10) of section 5a

$$\frac{F + D'}{\frac{1}{2} \rho\, V_0^2\, \pi\, R_t^2} = 2k\, \bar{w}_0 \left[1 - \bar{w}_0 \left(\frac{1}{2} + \frac{e}{k} \right) \right] \frac{R_\infty^2}{R_t^2} \qquad \dots\dots\dots\dots(6)$$

where $\bar{w}_0 = \dfrac{w_0}{V_0}$ and $V_0 - w_0$ is the axial velocity of the

windmill helical vortex sheets far downstream

and R_t is the outer radius of the windmill.

It should be noted that the values of e and k will be

different from their values for the unshrouded windmill due
to the presence of the vortex sheets in the bounding wake.
However no calculations of their values in this case are at
present available although presumably they could be obtained
by the experimental potential flow tank method suggested by
Theordorsen.[11]

Thus for a given value of the axial force, F, the
pressure drag D' and the effective radius of the slipstream,
R_∞, can be found.

The power output, P, from the windmill can be
obtained by equating it to the difference between the kinetic
energies of the fluid far upstream and far downstream of the
windmill less the work done by the pressures on the bounding
surfaces of the given control circuit.

Thus in the notation of section 5a,

$$P = \oint \left[p_o - p_1 + \frac{\rho}{2} (v_o^2 - q^2) \right] u_1 \, dS_\infty \quad \ldots\ldots\ldots (7)$$

where
$$u_1 = V_o + u_z$$
$$q^2 = u_r^2 + u_\theta^2 + (V_o + u_z)^2$$

But
$$p_o - p_1 = \rho w_o u_z + \rho q_1^2 / 2$$

where
$$q_1^2 = u_r^2 + u_\theta^2 + u_z^2$$

and if allowance for q, q_1 as functions of time are made then

$$P = \frac{\rho B}{H} \iiint \left[-u_z V_o (V_o - w_o) - u_z^2 (V_o - w_o) \right] dv \quad \ldots\ldots\ldots\ldots (8)$$

or

$$C_P = \frac{P}{\frac{1}{2}\rho V_o^3 \pi R_t^2} = 2k \, \bar{w}_o \, (1 - \bar{w}_o) \, \left(1 - \frac{e}{k} \bar{w}_o \right) \frac{R_\infty^2}{R_t^2} \quad \ldots\ldots\ldots\ldots (9)$$

which is identical with equation (12) of section 5a. The
correction for the drag of the blades is found from equation
(26) of section 5a. The value of R_∞ / R_t is found from the
duct calculations described above or approximately from
continuity. If the mean velocity increment in the plane of
the windmill due to the external duct is δV_2 then approximately

$$\frac{R_\infty^2}{R_t^2} \approx \frac{\left(1 - \frac{\bar{w}_o}{2} + \frac{\delta V_2}{V_o}\right)}{1 - \bar{w}_o} \qquad \ldots\ldots\ldots\ldots(10)$$

and

$$C_P \approx 2k\,\bar{w}_o\,\left(1 - \frac{e}{k}\bar{w}_o\right)\,\left(1 - \frac{\bar{w}_o}{2} + \frac{\delta V_2}{V_o}\right) \qquad \ldots\ldots\ldots\ldots(11)$$

If we put $k = e = 1$ and assume $\delta = \delta V_2/V_o$ is independent of $\bar{w}_o$ the maximum value of C_P occurs when

$$\bar{w}_o = \frac{3+2\delta - \sqrt{3 + 6\delta + 4\delta^2}}{3} \qquad \ldots\ldots\ldots\ldots(12)$$

As an example if $\delta = 2$, $\bar{w}_o = 0.48$ and $C_P = 1.38$ and similarly if $\delta = 1$, $\bar{w}_o = 0.46$ and $C_P = 0.89$.

These gains in power output are of the same order of magnitude as those calculated from one-dimensional theory and therefore justify to some extent the conclusions based on those results.

It must be stressed at this stage that C_P can only be determined when F, D', $\bar{w}_o$ and R_∞/R_t satisfy equation (6). Thus equation (6) is a compatability condition for these variables.

The experimental results obtained from ducted fans in streamlined fairings might at first sight be considered useful data in connection with the design of ducted windmills and so assist in formulating the accuracy of the above theoretical results. However due to differences in duct geometry and pressure gradients downstream of the windmill, the existing data can only be used qualitatively but if anything seem to confirm rather than contradict the above predictions.

6. The vortex theory of windmills

In section 5 the performance of the windmill has been analysed from a description of the vortex sheets, far downstream of the windmill, shed from its blades. In this way it was found unnecessary to specify the flow in the vicinity of the blades and the detailed blade geometry. However in making the assumption that the vortex sheets far

downstream are moving rearward as rigid helicoidal surfaces
a certain distribution of circulation along the blades is
implied. This in turn fixes the blade chord and blade pitch
angle as functions of radius, but this blade geometry is found
to be unsuitable for most practical applications. However
small changes in blade geometry from the ideal have been shown
not to affect materially the description of the vortex wake
far downstream. Hence the vortex sheets in the form of rigid
helicoidal surfaces represents a good approximation to the
vortex wake of a windmill of arbitrary design. It should be
pointed out, however, that the assumption that the vortex sheets
are in the form of rigid helicoidal surfaces is not essential
and an adequate theory can be built up in which helical
vortices of arbitrary strength are shed from each blade element.
The former assumption is, however, best suited to practical
applications.[7]

The theory, as discussed below, is equivalent to
the lifting line theory of aerofoils and will be adequate when
the aspect ratio and the distance between adjacent blades are
large. For blades of small aspect ratio lifting surface
theory will be necessary. It is not envisaged, for the case
of aerofoils of conventional design, that such elaboration of
the theory will prove necessary.

If the windmill rotates with angular velocity Ω in
a uniform flow of velocity V_o the lift on the elements of
each blade is a function of the local blade incidence i.e. the
angle between the blade chord line and the resultant velocity.
This lift must be associated with the circulation around the
blade element. But the circulation will vary from the tip
to the root of the blades and hence trailing vortices will
spring from the blades and pass downstream in helical paths
(see figure 14). In general the changes in circulation
along the blade will be greatest near the tips and the roots
and hence in these regions there will be strong concentrations
of vorticity. The induced velocities from the helical
vortices, in the slipstream downstream of the windmill, must
be evaluated in order that the true resultant velocity of the
fluid relative to the blades, and hence the true angle of
incidence, can be obtained. With this velocity and incidence
at each blade element and with the aid of the two-dimensional
characteristics of the blade section, the lift and drag
forces on the element can be found (see figure 15). Since in
general the induced velocities are periodic in character, the
lift and drag forces on the blade element are functions of
time. In this section only the mean values with respect to
time of the induced velocities will be considered.

6(a)   The unshrouded windmill

Since the axial component of the induced velocities is in the opposite direction to that of the wind far upstream (see figure 15) the slipstream downstream of the windmill must suffer an expansion.   Thus the helical vortices springing from the blades of the vortices must increase in diameter as they move downstream.   We assume that, for purposes of calculation only, far downstream of the windmill the vortex sheets do not roll up but continue to move away from the windmill in a regular manner.   On the assumption that the vortex sheets are of constant diameter far downstream of the windmill, the induced velocity at a given radius due to these moving vortex sheets can be calculated and hence the induced velocity at the corresponding radius in the plane of the blades can be found.   In practice the expansion of the vortex elements in the slipstream can usually be neglected.   The induced velocities are then calculated for a helical vortex of strength $-d\Gamma$ at radius r, having a pitch angle $\phi' = \tan^{-1}(V_o - w_o / \Omega r)$, where $(V_o - w_o)$ is the axial velocity of the vortex element relative to the windmill.   (The value of w_o, which is only independent of radius when the vortex moves as part of a rigid helicoidal surface, can, to a first approximation, be estimated with reasonable accuracy from the simple momentum theory formula for axial force or power).   When w_o is large, however, errors in the calculations of the induced velocity distribution in the plane of the blades will arise if the expansion of the vortex elements is neglected.   This effect will be discussed in section 6b below.

If $P'(x',y',z')$ is a point on the vortex of strength $-d\Gamma$ then the velocity induced d^2q at the point $P(r,0,o)$ in the plane of the windmill, due to the element of length ds of the vortex at P' is by Biot-Savart's law

$$d^2q = -\frac{d\Gamma}{4\pi}\frac{\sin\psi\,ds}{R^2} \qquad\qquad \ldots\ldots\ldots\ldots(1)$$

where $R = \overline{PP'}$ and ψ is the angle between $\overline{PP'}$ and ds. When we integrate over s from 0 to ∞, over all vortex sheets, and along the length of each blade and find the components of the induced velocity w_n and w_t perpendicular and parallel respectively to the resultant velocity we have

that[10]

$$w_n(r) = \frac{B\sqrt{(1+\mu^2)}}{4\pi\,\mu\,R_t}\,\mu_o\,\Gamma(\mu) + \frac{B\sqrt{(1+\mu^2)}}{4\pi\,\mu\,R_t}\,\mu_o\sum_{m=1}^{\infty}\int_{o}^{\mu}\,m\,B\mu'\,I'_{mB}(mB\mu')\,K_{mB}(mB\mu)$$

$$\times\;\;\frac{d\Gamma}{d\mu'}\,d\mu' + \frac{B\sqrt{1+\mu^2}}{4\pi\,\mu\,R_t}\,\mu_o\sum_{m=1}^{\infty}\int_{\mu}^{\mu_o}\,mB\mu'\,I_{Bn}(mB\mu)\,K'_{Bm}(mB\mu')\,\frac{d\Gamma}{d\mu'}\,d\mu'$$

$$\dots\dots\dots\dots(2)$$

$$w_t(r) = 0$$

where $\mu,\mu_o = \dfrac{r\,\Omega}{(V_o - w_o)}$, $\dfrac{R_t\,\Omega}{V_o - w_o}$ respectively

$$w_o(r) = 2w_n(r)\cos\phi'$$

B   number of blades

R_o outer radius

I,K   Bessel functions of the third kind

$I'(z)\;K'(z)$ $\dfrac{dI}{dz}$, $\dfrac{dK}{dz}$

If the effect of the boss is included $w_t(r)$ still equals zero but the normal induced velocity, $w_n(r)$ becomes,

$$w_n(r) = \frac{B\sqrt{1+\mu^2}}{4\pi\mu}\frac{\mu_o}{R_t}\,\Gamma(\mu) + \frac{B\sqrt{1+\mu^2}}{4\pi\,\mu\,R_t}\,\mu_o\sum_{m=1}^{\infty}\left\{\int_{\mu_1}^{\mu}m\,\mu'\left(I'_{Bm}(Bm\mu')K_{Bm}(Bm\mu)\right.\right.$$

$$\left.- \frac{K_{Bm}(Bm\mu')K'_{Bm}(Bm\mu')\,I'_{Bm}(Bm\mu_1)}{K'_{Bm}(Bm\mu_1)}\right)\;\frac{d\Gamma}{d\mu'}\,d\mu' \;\;\dots\dots\dots\dots(2a)$$

$$+ \int_{\mu}^{\mu_o}m\mu'K'_{Bm}(Bm\mu')\left[I_{Bm}(Bm\mu) - \frac{K_{Bm}(Bm\mu)I'_{Bm}(Bm\mu_1)}{K'_{Bm}(Bm\mu_1)}\right]\frac{d\Gamma}{d\mu'}\,d\mu'\right\}$$

where $\mu_1 = \dfrac{\Omega R_i}{V_o - w_o}$ and R_i is the boss radius.

A further increment in induced velocity arises from the flow

field around the boss. This can be estimated by the method described in section 5b(ii).

w_n and w_t are the components of the induced velocity in the plane of the windmill due to the trailing vortices and act normal to and in line with, respectively the velocity W'.
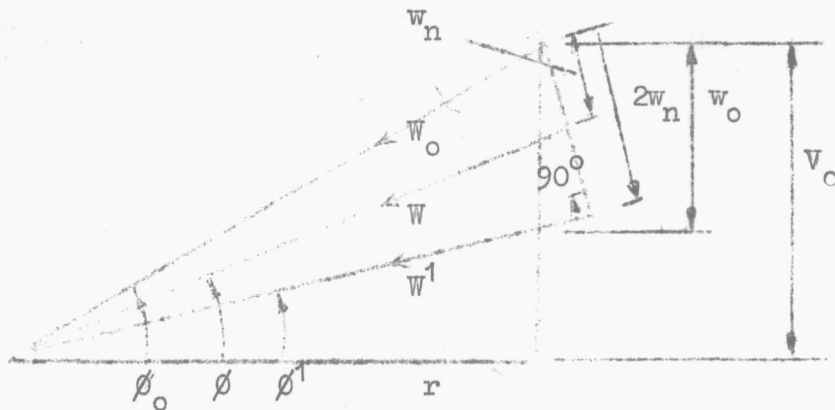
$$\phi' = \tan^{-1}\left(\frac{V_o - w_o}{\Omega r}\right) \qquad \text{pitch angle of vortex far downstream}$$

$2w_n$ resultant induced velocity far downstream normal to W'

w_n resultant induced velocity in plane of windmill (approximately normal to W).

In general no great loss in accuracy results if $w_n = w_1$ (see figure 1.) is assumed to act normal to the resultant velocity W. From the sketch above it can be seen that with the above approximation

$$W = \frac{V_o - w_o/2}{\sin \phi} + \frac{w_o}{2}\sin \phi \qquad \ldots\ldots\ldots\ldots(3)$$

The angle of incidence, a, of the blade at radius r is given by (see figure 1)

$$a = \phi - \theta \qquad \ldots\ldots\ldots\ldots(4)$$

where ϕ is the relative flow angle

and θ is the blade pitch angle relative to the plane of rotation.

The lift force per unit radius, L, acting on the blade at radius r is given by

$$L = \tfrac{1}{2}\rho W^2 c\, C_L = \rho\, \Gamma(r)\, W(r) \qquad \cdots\cdots\cdots(5)$$

where $\qquad C_L = a_o\,(a - a_o) \qquad\qquad\qquad \cdots\cdots\cdots(6)$

$a_o,\ a_o \qquad$ two dimensional lift curve slope and the no-lift angle of the aerofoil section

$c \qquad$ local blade chord

or, $\qquad \Gamma(r) = \dfrac{W c\, C_L}{2} \qquad\qquad \cdots\cdots\cdots(7)$

Equations (2) to (7) inclusive define an integral equation which can best be solved by a method of successive approximation.

In the design of airscrews Lock and Yeatman[7] have used, in place of equation (2), the corresponding values of w_n determined by Goldstein for the ideal airscrew. They tabulate a circulation function, K, as a function of $\sin\phi$, r/R_o, B, where K is defined from the relation

$$w_1 = \dfrac{\sigma\, a_o(\phi - \theta - a_o)}{4 \sin\phi\; K} \qquad \cdots\cdots\cdots(8)$$

where $\qquad \sigma = \dfrac{B\, c}{2\pi r} \qquad$ is the blade solidity.

In place of equation (8) Theordorsen[11] has found a relation between σC_L and $\bar{w}_o$, ϕ, B, and $V_o - w_o / n\, D_\infty$, which can be written

$$\sigma C_L = \dfrac{2\bar{w}_o\,(1-\bar{w}_o)}{(1-\bar{w}_o/2)\left(1 - \dfrac{\bar{w}_o \cos^2\phi}{2}\right)}\; K(x)\; \dfrac{\sin^2\phi}{\cos\phi} \qquad \cdots\cdots(9)$$

where $K(x) = \Gamma(x)\,\dfrac{B\,\Omega}{2\pi w_o}(V_o - w_o)$ is tabulated in reference 11.

and $\qquad \dfrac{K(x)}{\cos^2\phi}\dfrac{(1-\bar{\bar{w}}_o/2)}{(1-\bar{\bar{w}}_o)} = \mathcal{K}(x)$ corresponds to the

function tabulated by Lock and Yeatman[7].

When W and ϕ have been found for each radius the lift and drag forces can be calculated and by resolution the torque, Q, and axial force, F, can be obtained (see figure 14).

Hence

$$F = \frac{B\rho}{2}\int_{Boss}^{Tip} C_x \cos\phi \sin\phi\, c\bar{W}^2 dr \quad \ldots\ldots\ldots\ldots(10)$$

and

$$Q = \frac{B\rho}{2}\int_{Boss}^{Tip} C_y \cos\phi \sin\phi\, cr\,\bar{W}^2 dr \quad \ldots\ldots\ldots(11)$$

where

$$C_x = \frac{C_L}{\sin\phi} + \frac{C_D}{\cos\phi} = \frac{C_L}{\sin\phi}\left(1 + \frac{C_D}{C_L}\tan\phi\right)$$

$$C_y = \frac{C_L}{\cos\phi} - \frac{C_D}{\sin\phi} = \frac{C_L}{\sin\phi}\left(\tan\phi - \frac{C_D}{C_L}\right)$$

But from equation (3)

$$W = \frac{V_o - w_o/2}{\sin\phi} + \frac{w_o}{2}\sin\phi$$

hence

$$\frac{F}{\frac{1}{2}\rho V_o^2 \pi R_t^2} = \int_{Boss}^{Tip} C_x\,\sigma\cot\phi\left(1 - \frac{\bar{\bar{w}}_o\cos^2\phi}{2}\right)^2 dx^2 \ldots\ldots\ldots\ldots(12)$$

$$\frac{Q}{\frac{1}{2}\rho V_o^2 \pi R_t^3} = \int_{Boss}^{Tip} C_y\,\sigma\cot\phi\left(1 - \frac{\bar{\bar{w}}_o\cos^2\phi}{2}\right)^2 x\, dx^2 \ldots\ldots(13)$$

and since $P = \Omega Q$

$$\frac{P}{\frac{1}{2}\rho V_o^3 \pi R_t^2} = \frac{R_t\Omega}{V_o}\int_{Boss}^{Tip} C_y\,\sigma\cot\phi\left(1 - \frac{\bar{\bar{w}}_o\cos^2\phi}{2}\right)^2 x\, dx^2 \ldots(14)$$

where $\qquad x = r/R_t$; $\quad \sigma = Bc/2\pi r$; $\quad \bar{w}_o = w_o/V_o$

A more convenient expression for the power output coefficient can be found as follows. If the overall blade solidity, $\bar{\sigma}$, is given by

$$\bar{\sigma} = \frac{\int_{R_i}^{R_t} Bc \, dr}{\pi(R_t^2 - R_i^2)} \qquad \cdots\cdots\cdots\cdots(15)$$

and using the relations above for C_y and $\tan\phi$ then equation (14) becomes

$$C_P = \frac{P}{\frac{\rho}{2} V_o^3 \pi R_t^2} = \left(\frac{R_t \Omega}{V_o}\right)^2 \bar{\sigma} \int_{Boss}^{Tip} \frac{\sigma}{\bar{\sigma}} C_L \left(1 - \frac{C_D \, x \, \frac{\Omega R_t}{V_o}}{C_L \left(1 - \frac{\bar{w}_o}{2}\right)}\right) \frac{\left(1 - \frac{\bar{w}_o \cos^2\phi}{2}\right)^2}{\left(1 - \frac{\bar{w}_o}{2}\right)} x^2 dx^2$$

$$\cdots\cdots\cdots\cdots(16)$$

or

$$\frac{C_P}{\left(\frac{R_t \Omega}{V_o}\right)^2 \bar{\sigma} \, C_{L_{0.75}}} = \int_{Boss}^{Tip} \frac{\sigma}{\bar{\sigma}} \frac{C_L}{C_{L_{0.75}}} \left(1 - \frac{C_D \, x \, \frac{\Omega R_t}{V_o}}{C_L \left(1 - \frac{\bar{w}_o}{2}\right)}\right) \frac{\left(1 - \frac{\bar{w}_o}{2} \cos^2\phi\right)^2}{\left(1 - \frac{\bar{w}_o}{2}\right)} x^2 \, dx^2$$

$$\cdots\cdots\cdots\cdots(17)$$

From the experimental results of Iwasaki[4] the empirical relation between C_P, $\frac{\Omega R_t}{V_o}$, $\bar{\sigma}$ and $C_{L_{0.75}}$

is $\qquad C_P \xrightarrow{\quad} \frac{1}{4} \left(\frac{\Omega R_t}{V_o}\right)^2 \bar{\sigma} \, C_{L_{0.75}}$ $\qquad \cdots\cdots\cdots\cdots(18)$

where the factor 0.25 represents the approximate value of the integral on the right hand side of equation (17).

The difference in the performance of slow and fast running windmills can easily be demonstrated from the relations above.

The slow running windmill has a low value of $\mu_o = \Omega R_t/V_o$ (say 1 to 2) and a high solidity (large number of blades). The fast running windmill has a value of μ_o (between 3 and 6) and

a low solidity (small number of blades). The overall solidity $\bar{\sigma}$ in the former case is usually about 1.0 and 0.2 in the latter. Thus for a slow running windmill $\mu_o^2 \bar{\sigma}$ is about 1 whereas for a fast running windmill $\mu_o^2 \bar{\sigma}$ is about 2. On the other hand the torque is proportional to $\mu_o \bar{\sigma}$. Therefore the slow running windmill having values of $\mu_o \bar{\sigma}$ equal to about 1 has greater values than the fast running windmill whose value of $\mu_o \bar{\sigma}$ is about 0.6. This shows clearly why the slow running windmill is favoured in cases of light or variable wind.

6b. The ducted windmill

In section 5b the performance of the ducted windmill has been obtained from a consideration of the movement of the helical vortex sheets far downstream and the induced flow in the plane of the windmill imparted by the duct. In finding the local lift and drag forces acting on the blades the duct and the helical vortex sheet induced velocities must first be determined in the plane of the blades.

When the duct is of constant diameter and infinitely long the effect of the duct is to prevent the normal expansion of the slipstream downstream of the windmill. As a result the induced velocities in the plane of the blades arising from the vortex sheets downstream of the windmill are different from those of the unshrouded windmill due to this 'image effect'. The induced velocities far downstream superimposed on the uniform axial velocity will cause a variation of the axial velocity across the duct. This variation is in general quite significant and cannot justifiably be neglected.

For a duct of arbitrary shape the induced velocity, due to the duct alone, can be calculated by the method described in section 5b(ii). The method proposed for the calculation of the induced velocity in the plane of the blades due to the helical vortex sheets downstream of the windmill, follows from the fact that the induced velocities, in the plane of the windmill, are relatively insensitive to variations in the radius of the vortex elements far downstream. Thus although in the actual flow the vortex sheets must expand in diameter, together with their images in the boundary wall and the vortex sheets springingfrom the duct exit, it will

be assumed that they are of constant diameter operating inside
a constant diameter duct infinitely long. The calculation
of the induced velocities from the helical vortex sheets from
a windmill mounted in a duct of arbitrary shape is therefore,
to a first approximation, identical with that for a duct of
constant diameter.

The question now arises as to what pitch of the
helical vortex elements should be used. When w_o, the axial
displacement velocity of the vortex element, is small compared
with V_o this question is easily answered. It has been
shown in section 5 that the overall performance of an un-
shrouded windmill depends only on conditions in the ultimate
slipstream. Thus in the calculation of the induced velocities
between the vortex sheets far downstream of the windmill the
pitch of the vortex sheets must be based on $V_o - w_o$, the
axial displacement velocity of the vortex elements relative
to the windmill. Since w_o is assumed small compared with
V_o the diameter of the vortex elements far downstream are
only slightly greater than the corresponding elements at the
plane of the blades. In this case the induced velocity at
a given radius in the plane of the blades is very nearly
equal to half the calculated induced velocity, at the same
radius far downstream, in terms of the pitch of the vortex
sheets based on $V_o - w_o$. This clearly is the value to take
in the case of a ducted windmill when the duct is one of
constant diameter.

When w_o is not small compared with V_o the vortex
element expands as it moves downstream and in consequence its
pitch changes due to both the change in diameter and the axial
displacement velocity of the vortex element. If the induced
velocities in the plane of the blades are evaluated using the
Biot-Savart law allowing for this variation in diameter, it
can be shown, qualitatively, that the final result, as stated
above, is relatively insensitive to variations in the radius
of the vortex elements far downstream.

Thus in any approximate evaluation of the induced
velocities in the plane of the blades for large values of w_o,
the pitch of the vortex sheets just downstream of the windmill
should be used. In the case of the ducted windmill the pitch
of the vortex sheets should therefore be based on the axial
velocity, V_2, see section 5b.

In order to reduce the losses in the slipstream it
may prove advantageous to use guide vanes downstream of the

windmill at the entrance to the diffuser. It is unlikely that any great increase in power output will result from this cause since any gain in overall efficiency will be partly offset by the increased drag and by increased diffuser losses.

(i) Constant diameter duct

If V_o is the axial velocity of the uniform flow far upstream of the windmill, which is rotating with the angular velocity, Ω, then the elements of the B blades at a radius, r, will each shed helical vortices, of pitch angle $\phi_o = \tan^{-1}(V_o/\Omega r)$, into the main flow. The strength of these vortices will be $-d\Gamma$, where $-d\Gamma$ is the change in circulation around the blade element between radius r and $r + dr$. The equivalent induced velocity in the plane of the blades can be calculated using the Biot-Savart law and integrating over the complete length of the vortex as discussed in section 6a above. However since the helical vortices are moving inside a duct the images of the vortices outside the duct must also be considered in order to satisfy the boundary condition of zero normal (or radial) velocity at the duct boundary. A more direct method is to find a solution of the potential equation satisfying the appropriate boundary conditions.

In either case the components of the induced velocity[4,13] in the plane of the windmill are

$$w_n(r) = \frac{B\Omega\sqrt{1+\mu^2}}{4\pi V_o \mu}\Gamma(\mu) + \frac{B\Omega\sqrt{1+\mu^2}}{2\pi V_o \mu}\sum_{m=1}^{\infty}\left\{\int_0^{\mu}\mu'm\, I'_{Bm}(Bm\,\mu')\right.$$

$$\left[K_{Bm}(Bm\,\mu) - \frac{K'_{Bm}(Bm\,\mu_d)\,I_{Bm}(Bm\,\mu)}{I'_{Bm}(Bm\,\mu_d)}\right]\frac{d\Gamma}{d\mu'}\,d\mu'$$

$$+ \int_{\mu}^{\mu_o}\mu'm\left[K'_{Bm}(Bm\,\mu')I_{Bm}(Bm\,\mu) - \frac{K'_{Bm}(Bm\,\mu_d)\,I_{Bm}(Bm\,\mu)\,I'_{Bm}(\mu')}{I'_{Bm}(Bm\,\mu_d)}\right]\frac{d\Gamma}{d\mu'}\,d\mu'\right\}$$

$$\dotfill (1)$$

and $\qquad w_t(\mu) = 0$

where w_n and w_t are the components of the induced velocity perpendicular and parallel to the resultant velocity $\sqrt{V_o^2 + \Omega^2 r^2}$.

and $\quad \mu_o = \dfrac{\Omega R_t}{V_o}$, where R_t is the blade tip radius

$\quad\quad\quad\quad \mu_d = \dfrac{\Omega R_d}{V_o}$, where R_d is the duct radius.

Approximations to these expressions have been given by Iwasaki[4], where only the first term in the asymptotic expansions of the Bessel functions has been retained.

It should be noted that the axial velocity component far downstream of the windmill is not equal to V_o but is $V_o - w_o$, where $w_o \approx 2w_n \sec \emptyset_o$ $(\tan \emptyset_o = V_o/\Omega r)$. Clearly w_o is not constant with radius and must vary in magnitude and sign in order to satisfy the continuity relation. This feature has been neglected by most writers on the performance of axial flow windmills (or fans). Its neglect is only justified when the blade circulation is so adjusted that the magnitude of the radial velocity in the plane of the windmill, is very small.

In some cases a better approximation to w_n is required. This can be obtained from the first approximation to $w_o(r)$, on the assumption that the local pitch angle of the vortex far downstream is $\tan^{-1}(V_o - w_o/\Omega r)$ in place of $\tan^{-1}(V_o/\Omega r)$. Thus $w_n(r)$ can be determined from equation (1) with $\mu = \Omega r/V_o - w_o(r)$.

The procedure for finding the blade lift and drag, and hence the output power from the windmill, is identical with that described in section 6a above. It can easily be shown, however, that one important result of the windmill operating inside a duct is that the circulation, and therefore the lift, do not fall off so rapidly towards the tip as in the case of the unshrouded windmill. Iwasaki[4] has shown that the theoretical gain in power due to this cause alone can be as much as 15 per cent and experiments have confirmed this.

(ii) Duct of variable diameter

As stated above it will be assumed, in the calculation of the induced velocity distribution in the plane of the windmill due to the trailing helical vortex sheets, that the outside diameter of the sheets is equal to the outside diameter of the windmill and the vortex sheet diameter far downstream is equal to the duct diameter in the plane of the windmill. It is assumed that the axial velocity distribution across the plane of the windmill, due to the venturi effect of the duct, has been calculated, say, by the method discussed in section 5b(ii).

Thus the local velocity relative to the rotating blades has the components $\Omega r + w_n \sin \phi'$ and $V_o - w_n \cos \phi' + \delta V_2$, see figure 16, and the resultant velocity, W, and the relative flow angle, ϕ, both as functions of r/R_o can be determined once w_n is known.

The angle of incidence of the blades, a, is given by

$$a = \phi - \theta \qquad \dots\dots\dots\dots(2)$$

where $\tan \phi = (V_o - w_n \cos \phi' + \delta V_2) / (\Omega r + w_n \sin \phi')$ and the local circulation, Γ, in terms of the lift coefficient, C_L, is

$$\Gamma = \frac{W c C_L}{2} = \frac{W c}{2} a(\phi - \theta - a_o) \qquad \dots\dots\dots\dots(3)$$

where   c is the chord

         a is the lift curve slope

and a_o is the no-lift angle.

Equations (1) and (3) form an integral equation in terms of $w_n(r)$ which must be solved by a suitable approximate numerical method.

7. <u>Discussion</u>

Detailed calculations of the performance of ducted windmills based on vortex theory have not been given in this report since at this stage in the investigation concrete proposals for the most satisfactory geometries of the duct and blades have not yet been formulated. The vortex theory of ducted windmills has been presented in order to check qualitatively the conclusions obtained from simple one-dimensional theory and to form the basis for further theoretical and experimental studies.

The conclusions reached in section 4c that the power output of a ducted windmill can be arranged to be at least 65 per cent greater than that of an ideal unshrouded windmill of similar geometry appears, if anything, to be on the low side, although this figure corresponds to power outputs greater than that obtained experimentally by Sanuki[3] and Iwasaki[4] with fairly crude duct geometries. In both the latter experiments the gains in power output obtained with ducted windmills have been largely due to reduction in tip losses and blade unstalling and little or no effect from controlled diffusion. The evidence to date is not conclusive as to the relative merits of long diffusers having large expansion ratios and high duct losses and short ducts having small losses. In section 4c the numerical calculations show the need for high values of the diffuser expansion ratio and large negative pressure coefficients at the duct exit but no attempt has been made to find the corresponding internal and external duct profiles of the duct and to investigate whether or not the estimated losses are correct. The reason for this is that little detailed information is available on the flow of air through diffusers having free exits in which the velocity external to the diffuser flow is considerably greater than the mean internal velocity downstream of the exit. Under such conditions the 'diffuser efficiency' or pressure recovery is likely to be greater than in the case where the external velocity is zero. In addition the action of the windmill is to speed up the flow near the walls of the duct at the expense of the flow near the centre. Experiments by Collar[16] with a windmill mounted inside a wind tunnel diffuser have shown an appreciable improvement in the velocity distribution in the diffuser, although naturally in these experiments the upstream velocity was not uniform and therefore represent different conditions from those discussed here.

It can be assumed, on the basis of present knowledge, that, unless future experimental results prove to the contrary, the most suitable form of duct will consist of an entry and exit cone shaped to form an annular duct of "streamlined sections

in which the exit to throat area ratio is about 3.5 and the inlet area is made not greater than the exit area. The loss in performance with ducts of crude aerodynamic shape can only be determined from experiment.

In the structural design of ducts having large inlet and exit area ratios the duct must withstand not only the drag forces but also the inward radial forces, corresponding to the lift on an aerofoil. The latter forces have not been discussed in the text above although they can be immediately derived from a knowledge of the pressure distribution over the duct which, incidentally, is required in the calculation of the drag force. It has been stated in the text that this drag force is not equal to the drag of the duct when the windmill is removed. This is because the lower pressure behind the windmill acts on the walls of the duct and produces an extra drag. Although the duct develops a radial force the induced drag is zero since no trailing vortices are shed in a symmetrical flow.[15] When the duct is inclined at an angle to wind a real lifting force and pitching or yawing moment develop and, because there are now trailing vortices, an induced drag. It is probable that the magnitude of this pitching or yawing moment will play a very important part in the design of the supporting structure for a ducted windmill. The effect of duct incidence on the magnitude of the induced velocity in the plane of the windmill is quite small and Muttray[17] has found that it is appreciably constant over an incidence range of $\pm 10^{\circ}$.

It was also shown from the calculations of section 4c that the ducted windmill disc loading is, as a result of the increased axial velocity, lower than in the case of the corresponding unshrouded windmill. Since, in addition, the tip losses will be reduced and gust effects lessened the overall mechanical design of the ducted windmill should prove simpler than its unshrouded counterpart, and would therefore tend to offset the additional cost of the diffuser and ducting. The increased steadiness in the flow through the plane of the ducted windmill, as a result of the contraction effect of the inlet cone, will cause the rotational speed to be steadier than in the case of the unshrouded windmill. This should present some simplification to the speed control problem. From the experimental results of Iwasaki[4] and Sanuki[3] a two or three bladed windmill appears to be best suited for operation inside a duct. The values of $\Omega R_t/V_o$ corresponding to maximum power output are in the range 3.1 to 3.7

In order to confirm the above predictions and to

optimise the geometrical layout from the conflicting points of view of cost and aerodynamic efficiency it is suggested that a wind tunnel testing programme should be undertaken. The models could be tested at a Reynolds number of about 1/5th full scale and because of this scale effect would give slightly pessimistic results. Extrapolation to full scale could be done using existing data on the variation of diffuser efficiencies and skin friction effects with Reynolds number.

Gauze screens of various mesh sizes and gauges would be used in the plane of the windmill to represent any desired value of disc loading. Only one contraction section with a contraction ratio of about 1.5, as suggested by the calculations above, would need to be made. A range of diffusers, having different expansion ratios and cone angles, various external body shapes, and ejector arrangements could all be tested in turn. The results obtained from such an experimental programme would be a valuable contribution to the understanding of the ducted windmill problem.

After the completion of this experimental programme the path would then be clear to commence the detailed design of a windmill, by the methods discussed above, suitable for high performance operation inside the optimum duct. In the meantime the methods can be applied to the experimental results of Sanuki[3] and a comparison made between theory and experiment. It is expected that as a result of these calculations simple numerical methods will be evolved for the performance of ducted windmills similar to those used at present in the design of axial flow fans. It should be noted, however, that a method in which the variation of the axial induced velocity with radius is neglected is unlikely to yield reliable results for the performance in this case.

Conclusions

1. The performance and design of ducted windmills using one dimensional theory, including the effects of friction and the external flow over the duct, are presented.

2. The results of the one dimensional theory are compared with more elaborate methods based on the vortex theory of windmills and the aerodynamic performance of ducted bodies.

3. The aerodynamic loading on the blades is discussed and the differences in the induced velocity components between ducted and unshrouded windmills noted.

4.   Calculations based on the one dimensional theory
show that gains in power output of at least 65 per cent of the
maximum power output of the ideal unshrouded windmill can be
obtained when the windmill is shrouded with a duct of suitable
geometry.   The importance of the diffuser expansion ratio
and the negative pressure coefficient at the duct outlet on
the power output are discussed.

5.   The reduced disc loading and slight alleviation
of gustiness on the blades with the ducted windmill will, it
is suggested, partly offset the cost of the duct and supporting
structure.   The increased steadiness in the rotational speed
of the windmill is an important factor in favour of the ducted
windmill.

6.   In view of the lack of experimental data on ducted
bodies of the type required for high performance operation
of ducted windmills a series of suitable wind tunnel
experiments is suggested.   In these no windmill would be
used but its place taken by gauzes of different porosities
giving pressure drops equal to the windmill disc loading.

REFERENCES

No.   Author   Title, date, etc.

1.   Betz, A.   Wind-Energie und ihre Ausnutzung durch
                        Windmühlen.
                        Göttingen, 1926.

2.   Vezzani, R.   Un impianto aeroelettrico pilota di
                        media potenza con accumulo idrico di
                        pompaggio.
                        L'Elettrotecnica Vol. 37 No. 9 pp.398-419,
                                            1950.
                        (see Engineers' Digest, Vol. 12, No. 5,
                                            1951).

3.   Sanuki, M.   Studies on biplane wind vanes ventilator
                        tubes and cup anenometers.
                        Papers in Meteorology and Geophysics
                        (Japan) Vol. 1, No.2-4 pp.279-290,
                                            Dec.   1950.

4.   Iwasaki, M.   The experimental and theoretical
                        investigation of windmills.
                        Rep. Res. Inst. App. Mech. (Japan),
                        Vol. II, No. 8,   Dec.   1953.

5.　Lilley, G.M.　　　　Comm. to Electrical Res. Association,
　　　　　　　　　　　　England,　1952 (unpublished).

6.　Goldstein, S.　　　On the vortex theory of Airscrews.
　　　　　　　　　　　　Proc.Roy.Soc.(A) Vol.123, 1929.

7.　Lock, C.N.H., and Tables for use in an improved method
　　　Yeatman, D.　　　of airscrew strip theory calculation.
　　　　　　　　　　　　R. and M. 1674,　1935.

8.　Kramer, K.N.　　　　The induced efficiency of optimum
　　　　　　　　　　　　propellers having a finite number of
　　　　　　　　　　　　blades.
　　　　　　　　　　　　N.A.C.A. Tech. Memo. 884, 1939.

9.　Kawada, S.　　　　　Calculation of induced velocity by
　　　　　　　　　　　　helical vortices and its application
　　　　　　　　　　　　to propeller theory.
　　　　　　　　　　　　Rep.Aero.Res.Inst. Tokyo Imp. Univ.
　　　　　　　　　　　　No. 172, Jan. 1939.

10.　Moriya, T.　　　　On the integration of Biot-Savart's
　　　　　　　　　　　　law in propeller theory.
　　　　　　　　　　　　J.Soc.Aero.Sc. (Japan) Vol. 9, No. 89
　　　　　　　　　　　　p.1015, Sep. 1942.

11.　Theordorsen, T.　　Theory of Propellers,
　　　　　　　　　　　　McGraw-Hill, 1948.

12.　Abe　　　　　　　　On the theory of windmills.
　　　　　　　　　　　　Rep. Inst. of High Speed Mechanics
　　　　　　　　　　　　Tohoku Univ. Sendai Jan, Vol. 5 No.42
　　　　　　　　　　　　March,　1951.

13.　Takeyama, H.　　　Helical vortices and cylindrical
　　　　　　　　　　　　boundaries of circular cross-section.
　　　　　　　　　　　　J.Japan Soc. App. Mech. Vol.3, No.13
　　　　　　　　　　　　Jan.　1950.

14.　Glauert, H.　　　　Aerofoil and airscrew theory.
　　　　　　　　　　　　C. U. P., 1926.

15.　Küchemann, D.　　　Aerodynamics of Propulsion.
　　　　　　and　　　　　McGraw-Hill, 1953.
　　　　Weber, J.

16.　Collar, A.R.　　　The use of a freely rotating windmill
　　　　　　　　　　　　to improve the flow in a wind tunnel.
　　　　　　　　　　　　R. and M. 1866, 1938.

17.　Muttray, H.　　　　See reference 15 above.

Table 1, 2, 3 and 4.   Ducted Windmill Performance

Table 1a

$$C_{p_4} = 0 \ . \ \frac{\triangle H_2 + \triangle H_3}{\frac{1}{2}\rho V_2^2} = 0.1$$

$1/\mu$	2	3	4	5
h_2	0.35	0.21	0.16	0.14
$C_{P_{max}}$	0.65	0.84	0.96	1.07
$r = \dfrac{C_{P_{max}}}{C_{P'_{max}}}$	1.10	1.42	1.62	1.81
L	0.35	0.21	0.16	0.14
$v = \dfrac{V_2}{V_o}$	0.98	1.26	1.45	1.61

Diffuser Expansion Ratio

$$\frac{S_3}{S_2} = \frac{1}{\mu}$$

$$h_2 = 0.1 + \mu^2$$

r = Performance Factor

$$L = \frac{\left(f_{at\ C_{P_{max}}}\right)_{Ducted}}{\left(f_{at\ C_{P_{max}}}\right)_{Free}}$$

= Disc loading ratio

v = Velocity ratio

Table 1b

$$C_{p_4} = 0 \quad \frac{\triangle H_2 + \triangle H_3}{\frac{1}{2}\rho V_2^2} = 0.15$$

$1/\mu$	2	3	4	5
h_2	0.40	0.26	0.21	0.19
$C_{P_{max}}$	0.61	0.76	0.84	0.89
r	1.03	1.28	1.42	1.50
L	0.40	0.26	0.21	0.15
v	0.91	1.14	1.26	1.34

Table 1c

$$C_{p_4} = 0 \quad \frac{\triangle H_2 + \triangle H_3}{\frac{1}{2}\rho V_2^2} = 0.20$$

$1/\mu$	2	3	4	5
h_2	0.45	0.31	0.26	0.24
$C_{P_{max}}$	0.57	0.69	0.76	0.79
r	0.97	1.17	1.28	1.33
L	0.45	0.31	0.26	0.20
v	0.86	1.04	1.14	1.19

Table 1d

$$C_{p_4} = 0 \qquad \frac{\Delta H_2 + \Delta H_3}{\frac{1}{2}\rho V_2^2} = 0.25$$

$1/\mu$	2	3	4	5
h_2	0.50	0.36	0.31	0.29
$C_{P_{max}}$	0.55	0.64	0.69	0.71
r	0.93	1.09	1.17	1.21
L	0.50	0.36	0.31	0.29
v	0.82	0.96	1.04	1.06

Table 2a

$$C_{p_4} = -0.10 \qquad \frac{\Delta H_2 + \Delta H_3}{\frac{1}{2}\rho V_2^2} = 0.10$$

$1/\mu$	2	3	4	5
r	1.27	1.63	1.86	2.08
v	1.03	1.33	1.52	1.70

Note: Values of h_2 and L are unchanged from their values with $C_{p_4} = 0$ above.

Table 2b

$$C_{p_4} = -0.10 \qquad \frac{\Delta H_2 + \Delta H_3}{\frac{1}{2}\rho V_2^2} = 0.15$$

$1/\mu$	2	3	4	5
r	1.19	1.47	1.64	1.73
v	0.96	1.19	1.32	1.41

Table 2c

$$C_{p_4} = -0.10 \qquad \frac{\Delta H_2 + \Delta H_3}{\frac{1}{2}\rho V_2^2} = 0.20$$

$1/\mu$	2	3	4	5
r	1.11	1.35	1.48	1.53
v	0.91	1.09	1.20	1.25

Table 2d

$$C_{p_4} = -0.10 \qquad \frac{\Delta H_2 + \Delta H_3}{\frac{1}{2}\rho V_2^2} = 0.25$$

$1/\mu$	2	3	4	5
r	1.07	1.26	1.35	1.40
v	0.86	1.01	1.09	1.11

Table 3a

$$C_{p_4} = -0.20 \qquad \frac{\Delta H_2 + \Delta H_3}{\frac{1}{2}\rho V_2^2} = 0.1$$

$1/\mu$	2	3	4	5
r	1.44	1.86	2.12	2.37
v	1.07	1.38	1.59	1.76

Table 3b

$$C_{p_4} = -0.20 \qquad \frac{\Delta H_2 + \Delta H_3}{\frac{1}{2}\rho V_2^2} = 0.15$$

$1/\mu$	2	3	4	5
r	1.35	1.68	1.86	1.97
v	1.00	1.25	1.38	1.47

Table 3c

$$C_{p_4} = -0.20 \qquad \frac{\Delta H_2 + \Delta H_3}{\frac{1}{2}\rho V_2^2} = 0.20$$

$1/\mu$	2	3	4	5
r	1.28	1.53	1.68	1.74
v	0.94	1.14	1.25	1.30

Table 3d

$$C_{p_4} = -0.20 \qquad \frac{\Delta H_2 + \Delta H_3}{\frac{1}{2}\rho V_2^2} = 0.25$$

$1/\mu$	2	3	4	5
r	1.22	1.43	1.53	1.58
v	0.90	1.05	1.14	1.16

Table 4a

$$C_{p_4} = -0.30 \qquad \frac{\Delta H_2 + \Delta H_3}{\frac{1}{2}\rho V_2^2} = 0.10$$

$1/\mu$	2	3	4	5
r	1.63	2.10	2.40	2.68
v	1.16	1.44	1.65	1.84

Table 4b

$$C_{p_4} = -0.30 \qquad \frac{\Delta H_2 + \Delta H_3}{\frac{1}{2}\rho V_2^2} = 0.15$$

$1/\mu$	2	3	4	5
r	1.53	1.90	2.10	2.22
v	1.04	1.30	1.44	1.53

Table 4c

$$C_{p_4} = -0.30 \qquad \frac{\Delta H_2 + \Delta H_3}{\frac{1}{2}\rho V_2^2} = 0.20$$

$1/\mu$	2	3	4	5
r	1.44	1.73	1.90	1.97
v	0.98	1.19	1.30	1.36

<u>Table 4d</u>

$$C_{p_4} = -0.30 \qquad \frac{\Delta H_2 + \Delta H_3}{\frac{1}{2}\rho V_2^2} = 0.25$$

$1/\mu$	2	3	4	5
r	1.38	1.61	1.73	1.79
v	0.93	1.10	1.19	1.21

<u>Table 5</u>

$$\frac{\Delta H_2 + \Delta H_3}{\frac{1}{2}\rho V_2^2} = 0 \qquad \text{Values of } r = \frac{C_{P_{max}}}{C'_{P_{max}}}$$

C_{p_4} \ $1/\mu$	2	3	4	5
0	1.30	1.95	2.60	3.25
-0.1	1.50	2.26	3.00	3.76
-0.2	1.71	2.56	3.42	4.27
-0.3	1.92	2.88	3.84	4.81
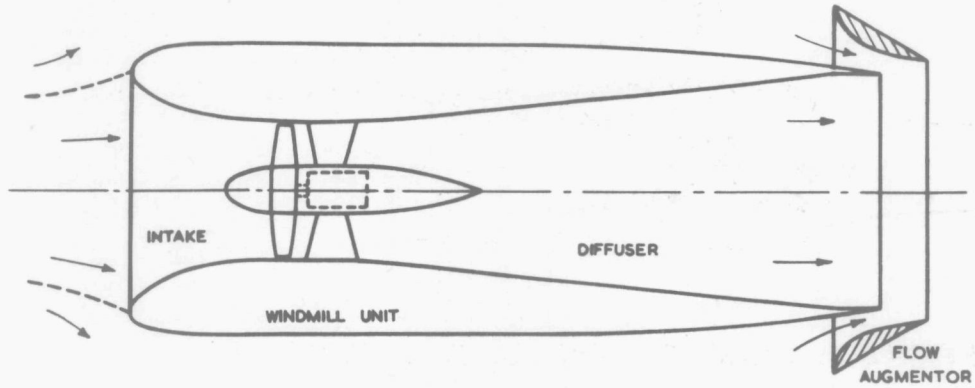
FIG. I. LAYOUT OF DUCTED WINDMILL
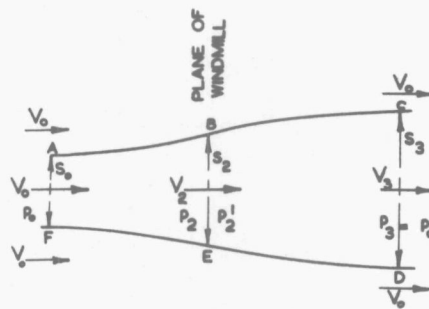
FIG. 2. DIAGRAM OF THE FLOW FIELD OF AN
UNSHROUDED WINDMILL
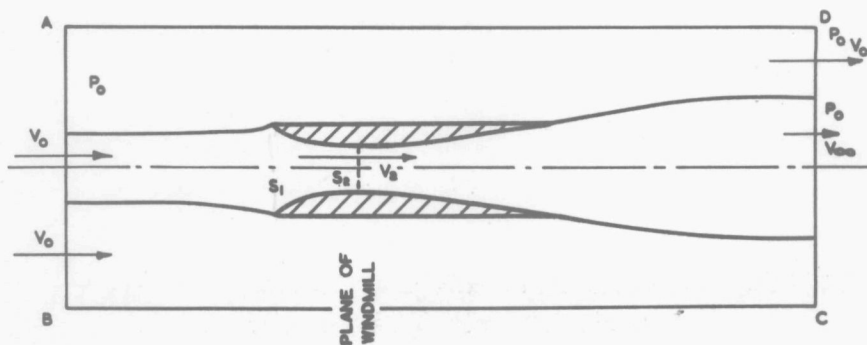
FIG. 3. CONTROL SURFACE FOR THE DUCTED WINDMILL
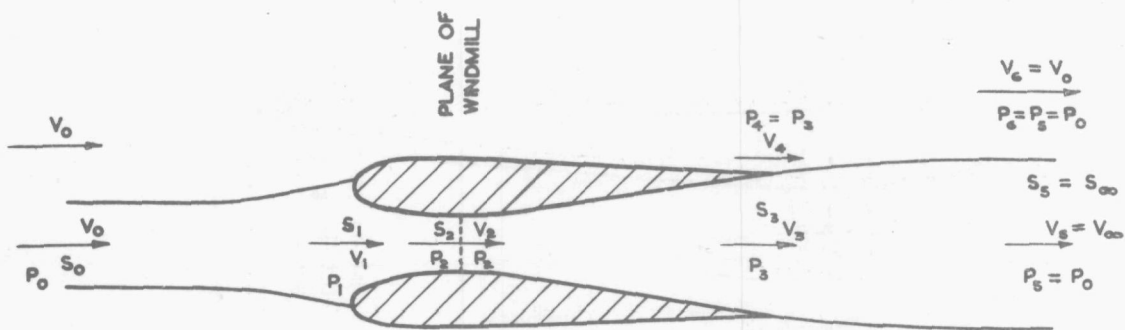
FIG. 4. DIAGRAM OF THE DUCTED WINDMILL
SHOWING THE INTERNAL AND EXTERNAL FLOW
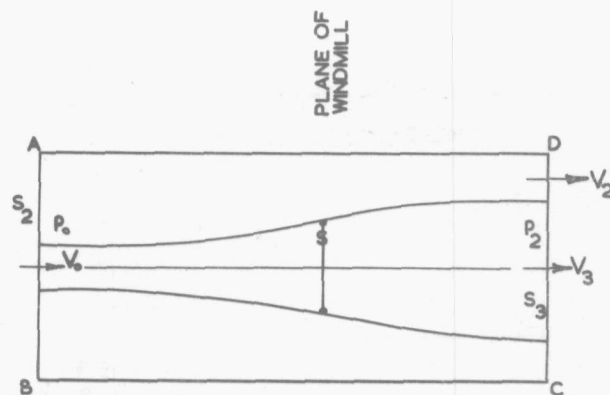
FIG. 5. CONTROL SURFACE FOR WINDMILL INSIDE A DUCT
EFFECT OF TIP CLEARANCE
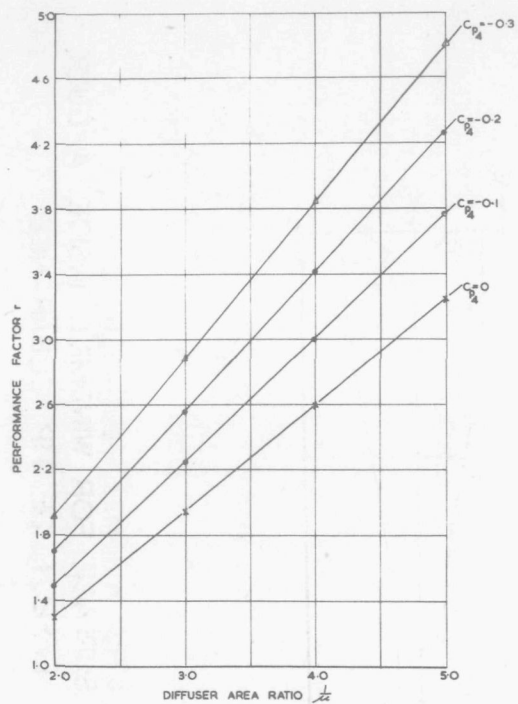
FIG. 6. DUCTED WINDMILL PERFORMANCE

Internal Loss Factor $\dfrac{\Delta H_2 + \Delta H_3}{\frac{1}{2}\rho\, V_2^2} = 0$
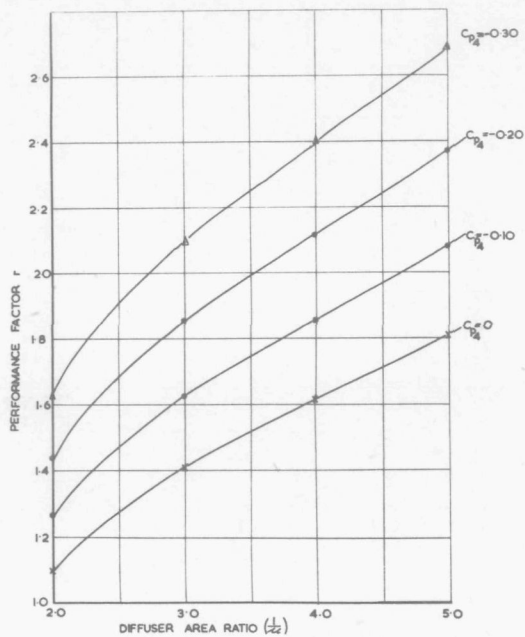
FIG. 7. DUCTED WINDMILL PERFORMANCE

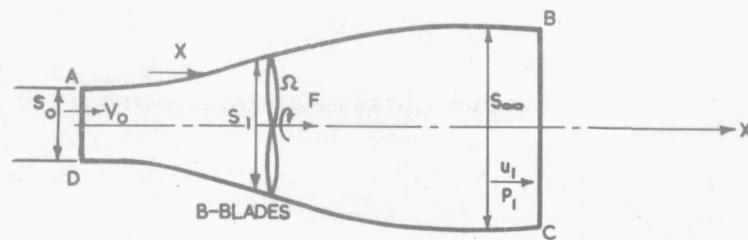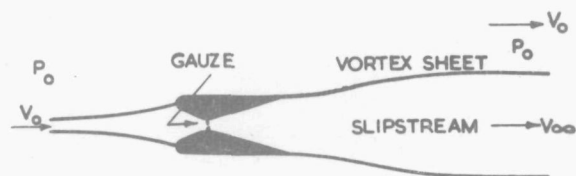$$\dfrac{\Delta H_2 + \Delta H_3}{\frac{1}{2}\rho\, V_2^2} = 0\cdot 10$$
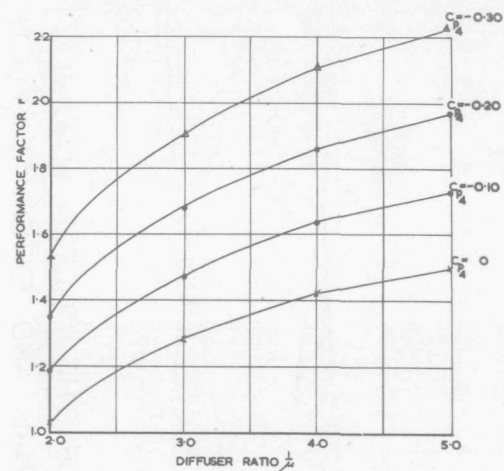
FIG. 8. DUCTED WINDMILL PERFORMANCE

$$\dfrac{\Delta H_2 + \Delta H_3}{\frac{1}{2}\rho\, V_2^2} = 0\cdot 15$$
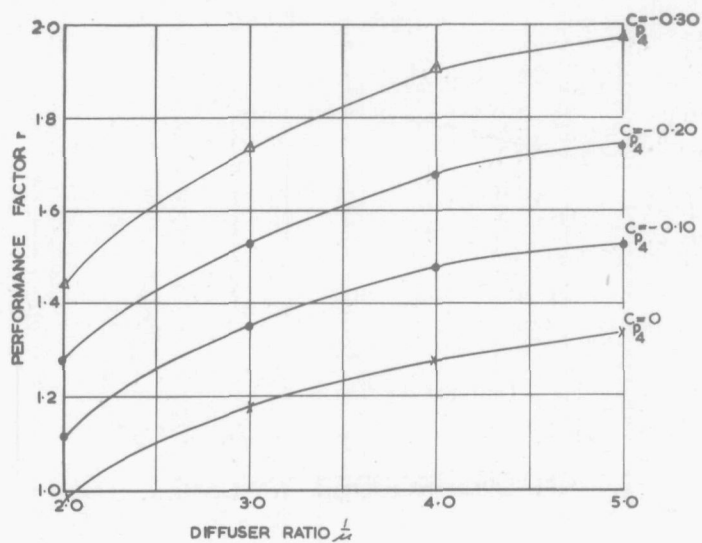
FIG. 9. DUCTED WINDMILL PERFORMANCE

$$\frac{\Delta H_2 + \Delta H_3}{\frac{1}{2}\rho V_2^2} = 0.20$$
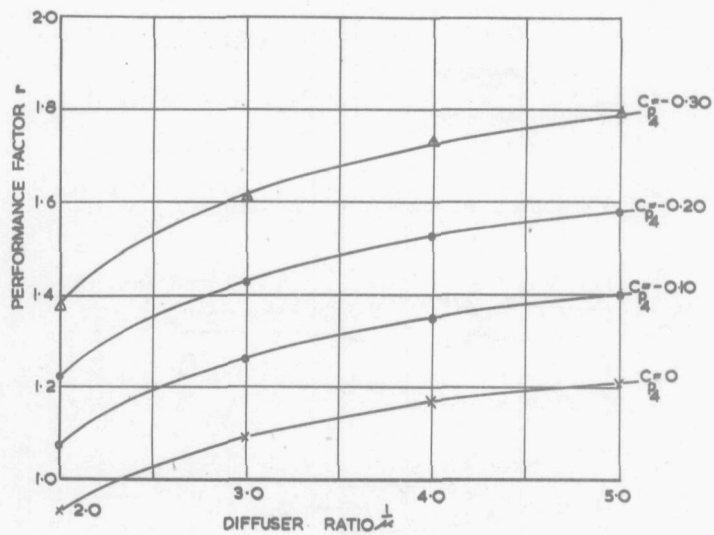
FIG. 10. DUCTED WINDMILL PERFORMANCE

$$\frac{\Delta H_2 + \Delta H_3}{\frac{1}{2}\rho V_2^2} = 0.25$$
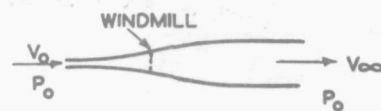
FIG. II. DIAGRAM OF THE FLOW PAST
AN UNSHROUDED WINDMILL

(1.) WINDMILL REPLACED BY A GAUZE

(2) DUCT ALONE

(3.) WINDMILL ALONE

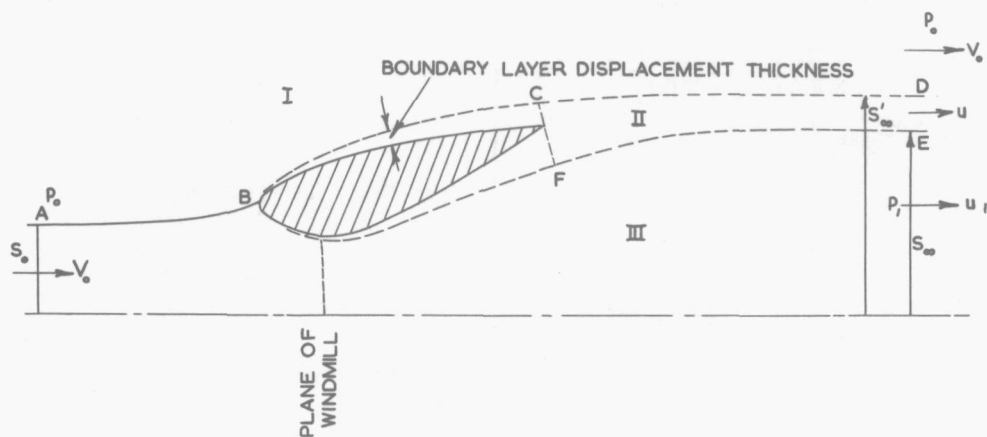FIG 12. GEOMETRY OF THE SLIPSTREAM
OF A DUCTED WINDMILL

BOUNDARY LAYER DISPLACEMENT THICKNESS

FIG. 13. CONTROL SURFACES FOR THE FLOW
PAST A DUCTED WINDMILL

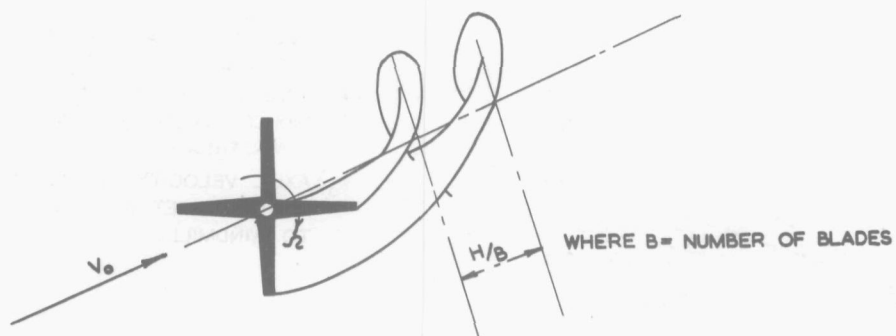

WHERE B = NUMBER OF BLADES

FIG. 14. THE HELICAL VORTEX SHEETS
DOWNSTREAM OF A WINDMILL

$$\Delta \text{ (AXIAL FORCE)} = B \left(\Delta \text{ (LIFT)} \cos \phi + \Delta \text{ (DRAG)} \sin \phi \right)$$

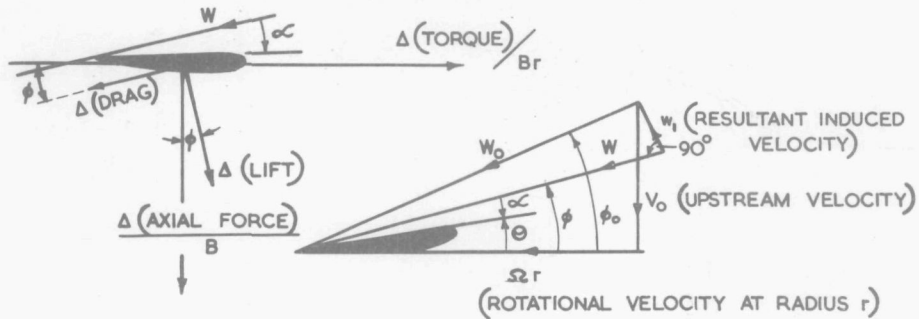$$\Delta \text{ (TORQUE)} = Br \left(\Delta \text{ (LIFT)} \sin \phi - \Delta \text{ (DRAG)} \cos \phi \right)$$

FIG. 15. DIAGRAM SHOWING VELOCITY COMPONENTS AND FORCES ACTING ON BLADE ELEMENT AT RADIUS r. (B = NUMBER OF BLADES)

δV_2 VELOCITY INCREMENT DUE TO DUCT.

$2w_n$ NORMAL COMPONENT OF INDUCED VELOCITY FAR DOWNSTREAM.

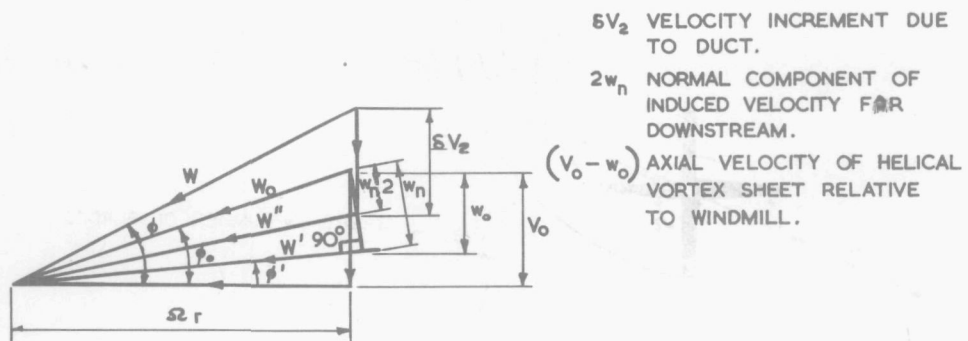$(V_0 - w_0)$ AXIAL VELOCITY OF HELICAL VORTEX SHEET RELATIVE TO WINDMILL.

FIG. 16. VELOCITY DIAGRAM SHOWING VELOCITY COMPONENTS DUE TO THE DUCT AND WINDMILL VORTEX SHEETS